

RESEARCH

Open Access



α -Synuclein purification significantly impacts seed amplification assay performance and consistency

Zaid A. M. Al-Azzawi^{1†}, Nicholas R. G. Silver^{2,3†}, Surabhi Mehra², Simeng Niu¹, Christopher Situ², Wen Luo^{1,4}, Irina Shlaifer^{1,4}, Martin Ingelsson^{2,5,6,7,8}, Bradley T. Hyman^{9,10,11}, Jean-François Trempe¹², Thomas M. Durcan^{1,4}, Joel C. Watts^{2,3*} and Edward A. Fon^{1*}

Abstract

α -Synuclein seed amplification assays are a promising diagnostic tool for synucleinopathies such as Parkinson's disease and multiple system atrophy. Standardized conditions are required to ensure a high degree of inter- and intra-laboratory reproducibility when performing these assays. A significant issue that hinders the utility of seed amplification assays is the *de novo* aggregation propensity of the α -synuclein substrate as well as inter-batch heterogeneity. While much work has focused on determining appropriate seed amplification assay buffer compositions as well as the type and amount of seed used, a robust comparison of α -synuclein substrate purification methods has not been reported. We therefore compared the utility of recombinant α -synuclein purified using four different methods as seed amplification assay substrates across two laboratories. Osmotic shock-purified α -synuclein monomer substrate showed the lowest propensity for *de novo* aggregation, which translated into being the best substrate for seed amplification assay reactions seeded with α -synuclein preformed fibrils or patient brain homogenates. Furthermore, osmotic shock α -synuclein monomer showed the best inter-batch reproducibility compared to all other substrates tested. As α -synuclein seed amplification assays continue to evolve and move towards adoption in the clinical realm, this work showcases the vital importance of standardizing the production and characterization of recombinant α -synuclein substrate. We encourage the widespread adoption of osmotic shock α -synuclein monomer as the universal substrate for seed amplification assays to maximize intra- and inter-laboratory reproducibility.

Keywords Neurodegenerative diseases, Diagnostics, Prions, RT-QuIC, PMCA, α -Synuclein, Purification, Osmotic shock

[†]Zaid A. M. Al-Azzawi and Nicholas R. G. Silver have contributed equally to this work.

*Correspondence:
Joel C. Watts
joel.watts@utoronto.ca
Edward A. Fon
ted.fon@mcgill.ca

Full list of author information is available at the end of the article



© The Author(s) 2025. **Open Access** This article is licensed under a Creative Commons Attribution-NonCommercial-NoDerivatives 4.0 International License, which permits any non-commercial use, sharing, distribution and reproduction in any medium or format, as long as you give appropriate credit to the original author(s) and the source, provide a link to the Creative Commons licence, and indicate if you modified the licensed material. You do not have permission under this licence to share adapted material derived from this article or parts of it. The images or other third party material in this article are included in the article's Creative Commons licence, unless indicated otherwise in a credit line to the material. If material is not included in the article's Creative Commons licence and your intended use is not permitted by statutory regulation or exceeds the permitted use, you will need to obtain permission directly from the copyright holder. To view a copy of this licence, visit <http://creativecommons.org/licenses/by-nc-nd/4.0/>.

Introduction

α -Synuclein (α Syn), encoded by the *SNCA* gene, is a pre-synaptic 140 amino-acid neuronal protein. While α Syn's native function remains unclear, its aggregation is a pathological hallmark of several neurodegenerative diseases known collectively as synucleinopathies, which include Parkinson's disease (PD), multiple system atrophy (MSA), and dementia with Lewy bodies (DLB) [71]. Seed amplification assays (SAAs) have drawn considerable attention recently as a promising diagnostic tool for synucleinopathies [7, 70]. SAAs are relatively easy and cost-efficient to perform, requiring only basic laboratory technology such as a fluorescence plate reader and inexpensive, non-hazardous chemicals that are readily accessible [20]. In their most basic form, SAAs consist of recombinant α Syn incubated under specific temperature and buffer conditions with a small amount of a seed-containing biospecimen. Due to the prion-like nature of α Syn aggregates [74], if the biospecimen contains an α Syn aggregate seed, natively-folded recombinant α Syn monomers will be recruited by the aggregate to undergo template-directed misfolding, resulting in propagation of the aggregate structure. The kinetics of the accumulation of aggregated α Syn can be tracked in real time using the fluorescent amyloid-binding dye Thioflavin T (ThT), which selectively fluoresces when it binds to β -sheet-rich regions in protein aggregates [80].

The first publications on the use of α Syn SAA in patient cohorts compared cerebrospinal fluid (CSF) samples from PD and DLB patients to Alzheimer's disease patients and healthy controls [25, 65]. In these initial reports, it was demonstrated that SAAs can be useful in the diagnosis of synucleinopathy patients. Indeed, the presence of α Syn seeding activity in CSF is now considered to be part of the biological definition of PD [33, 66]. With further developments it has been possible to reduce the duration required to run SAAs, from durations greater than a week to only a day [52]. The specificity and sensitivity of SAAs for synucleinopathies have also been improved, with some studies reaching up to 100% and 97%, respectively [4, 11, 12, 14, 15, 22, 31, 35, 43, 48, 54, 57–59, 69]. Furthermore, it has recently been shown that SAAs may have prognostic and not solely diagnostic value, and can be used to quantify α Syn seeds in patient biospecimens [9, 12, 14, 21, 49, 51, 72]. In addition to CSF, SAAs have also been used to detect α Syn seeding activity in serum, skin, olfactory mucosa, and urine samples from synucleinopathy patients [16, 22, 50, 78].

Individual laboratories have published their own SAA protocols, with slight variations in the buffer and incubation parameters required for enabling the efficient detection and amplification of α Syn aggregates from specific biospecimens [4, 11, 12, 14, 15, 18, 22, 31, 35, 43, 46–48, 54, 57–59, 69]. Some studies have found high

concordance in SAA results obtained across multiple laboratories [13, 36, 60]. However, as the field has progressed, the importance of standardizing assay conditions has become evident if SAAs are to be adopted for wider clinical use [8, 17, 37, 44, 73].

While the binary (yes/no) detection of α Syn aggregates can be comparable between protocols, the aggregation kinetics can be highly dependent on the conditions of the assay and the disease context [37, 60]. Whereas α Syn aggregation is a shared phenomenon across synucleinopathies, their clinical manifestation, neuropathological features, and progression are distinct. The conformational strain hypothesis postulates that each unique synucleinopathy can be attributed to a unique structural conformation of α Syn aggregate, which is supported by current neuropathological, biochemical and structural studies [42, 68]. Distinguishing between α Syn structural conformations using SAA aggregation kinetics could facilitate the diagnosis of specific synucleinopathies. Some studies have been able to distinguish PD from MSA using patient CSF and brain samples via the maximal ThT fluorescence value and/or the lag time required for the fluorescent signal to increase [41, 64]. Subsequent structural and biochemical characterization confirmed these aggregated SAA end-products to be different structural polymorphs [64]. Other studies have been able to find differences in aggregation kinetics between α Syn strains, however, they often find opposite effects, which may be due to use of different SAA conditions and parameters, highlighting the lack of standardization [18, 48, 79].

Some studies have investigated the effects of different buffer conditions and incubation parameters on SAA aggregation kinetics [1, 48]. In addition, it has been noted that variability exists between different batches of recombinant α Syn [12, 14, 37]. However, no studies have considered the effects the recombinant α Syn purification protocol could have on the SAA kinetics, despite purification methods being a known factor that affects α Syn aggregation propensity [1, 75].

Currently, multiple different recombinant α Syn purification protocols are used when generating the monomeric α Syn substrate for SAA [3, 11, 15, 54, 56, 64, 69]. The implicit assumption is that the properties of recombinant α Syn produced do not vary significantly between protocols or that any effects of the purification method chosen would be overridden by the buffer conditions used. To test these assumptions, we compared recombinant α Syn purified by three different methods as well as a commercially sourced recombinant α Syn as substrates for SAA. The *de novo* and seeded aggregation kinetics of the four substrates were tested using SAA under standardized conditions at two different laboratory sites. We found that recombinant α Syn purified using an osmotic shock protocol serves as the most robust SAA substrate,

with low rates of *de novo* protein aggregation and high inter-lab reproducibility.

Materials and methods

Purification of GST-tagged α Syn monomer

Glutathione S-transferase (GST)-tagged α Syn was purified as previously published [45]. A plasmid encoding GST-tagged full-length recombinant human α Syn (NM_000345) was transformed into BL21(DE3) *Escherichia coli* (New England Biolabs). When bacterial cultures reached an $OD_{600} > 0.6$, α Syn expression was induced using 1 M isopropyl β -D-1-thiogalactopyranoside (IPTG). Induction was performed overnight, after which cultures were centrifuged at $5000 \times g$ at 4 °C for 30 min. Pellets were resuspended in cold resuspension buffer (25 mM Tris-HCl pH 8, 400 mM NaCl, 5% glycerol, 0.5% Triton X-100, 5 mM PMSE, 0.5 mg/mL benzamidine, 0.5 μ g/mL leupeptin, 0.5 μ g/mL aprotinin, and 1 mM DTT). Resuspended pellets were then sonicated in an ice bath (5 cycles of 30 s ON/30 s OFF, 60% power). Next, the lysed pellets were centrifuged for 30 min at 18,000 rpm and 4 °C. Cleared lysates were filtered using a 0.2 μ m syringe filter (VWR) and then incubated with 5 mL of glutathione Sepharose beads (GE Healthcare Life Sciences) for at least 24 h.

GST-tagged α Syn was purified using 10 mL disposable chromatography columns (Thermo Scientific) and eluted using 20 mL of freshly prepared cold elution buffer (50 mM Tris-HCl pH 8, 400 mM NaCl, 5% glycerol, 1 mM DTT, and 20 mM glutathione). Eluents were combined into an Amicon Ultra-15 centrifugal filter unit and centrifuged at $4,000 \times g$ at 4 °C for 30 min. Filtrate containing purified GST-tagged synuclein was re-suspended using 10 mL of 1X PBS and re-concentrated until the final volume of eluent was ≤ 4 mL.

GST-tagged recombinant 3C enzyme, which cleaves the GST tag from GST-tagged proteins, was expressed and purified similarly. To cleave the GST tag, GST-3C protease was added to GST- α Syn at a 1:50 mass-to-mass ratio and mixed at 4 °C overnight. Removal of the GST tag leaves 5 N-terminal linker residues on the GST-cleaved α Syn. The mixture was injected into a GSTrap 4B column (GE Healthcare Life Sciences) and the flow-through was collected into a 50 mL tube. The flow-through containing GST-cleaved α Syn was then concentrated again by centrifuging at $4,000 \times g$ at 4 °C for 30 min using an Amicon Ultra-15 centrifugal filter unit to a volume of ≤ 4 mL. Finally, concentrated eluent was purified using a Superdex 200 16/600 column (GE Healthcare Life Sciences) on the ÄKTA pure L system (GE Healthcare Life Sciences). The desired sample fractions were collected into an Amicon Ultra-15 Centrifugal Filter Unit, centrifuged at 3,000 rpm and 4 °C for 10 to 15 min, and adjusted to a concentration of 5 mg/mL using sterile 1X PBS. Before

aliquoting into sterile tubes and freezing at -80 °C, purified α Syn was sterilized using a 0.2 μ m syringe filter.

Purification of α Syn monomer using osmotic shock

Full-length, untagged human α Syn was cloned into a pET-28a vector, expressed and purified from *E. coli* Rosetta 2 (DE3) bacteria (Novagen) using a modified osmotic shock and anion exchange protocol as follows [34, 38, 53]. When bacterial cultures reached an $OD_{600} > 0.6$, α Syn expression was induced using IPTG for a minimum of 3 h. Next, the cells were pelleted by centrifugation at $5,000 \times g$ for 15 min at 4 °C. The cell pellet was then washed in 1X PBS and spun down using the same centrifugation parameters.

The pellet was resuspended in osmotic shock buffer (30 mM Tris-HCl pH 7.2, 40% sucrose, and 2 mM ethylenediaminetetraacetic acid (EDTA)) at 100 mL of osmotic shock buffer per 1000 mL of bacteria culture used. Following a 10 min incubation at room temperature, the suspension was centrifuged at $9,000 \times g$ for 20 min at 20 °C. The supernatant was discarded, and the pellet was quickly resuspended in ice-cold dH₂O (40 mL per 1000 mL of bacteria culture used) after which saturated MgCl₂ (2.35 g/L) was added (40 μ L per 100 mL of bacterial cell suspension) and allowed to incubate on ice for 3 min. The suspension was then centrifuged at $9,000 \times g$ for 30 min at 4 °C and the supernatant was carefully collected.

Supernatant was filtered through a 0.22 μ m PES filter (FroggaBio) and dialyzed into 50 mM Tris-HCl pH 8.3 using 10 K MWCO SnakeSkin Dialysis Tubing (Thermo Scientific, #68100) overnight at 4 °C. α Syn was first purified via fast protein liquid chromatography using a HiPrep Q HP 16/10 (Cytiva) anion exchange column and eluted using a linear gradient of 0 to 500 mM NaCl in 50 mM Tris-HCl pH 8.3. Fractions were assessed for purity using sodium dodecyl sulfate polyacrylamide gel electrophoresis (SDS-PAGE) and Coomassie blue staining, with fractions showing sufficiently pure α Syn being pooled and re-dialyzed into 50 mM Tris-HCl pH 8.3 overnight at 4 °C. Coomassie blue stain was produced using Brilliant Blue Dye (BioRad) ethanol, glacial acetic acid (BioRad) and dH₂O. Dialyzed pooled fractions were further purified using a MonoQ anion exchange column (GE Healthcare) and eluted using the same linear gradient. Fractions were once again assessed for purity using 10% SDS-PAGE gels (Invitrogen, #NP0301BOX) and Coomassie blue staining. Fractions containing pure α Syn were dialyzed into dH₂O. Concentrations of α Syn were determined by measuring absorbance at 280 nm using a NanoDrop spectrophotometer (extinction coefficient = 5,960). The protein was aliquoted into 200 μ L aliquots, flash frozen in liquid nitrogen, and stored at -80 °C.

Purification of α Syn monomer using sonication and boiling

The same bacteria, induction and harvesting procedure used in the osmotic shock protocol was replicated for the sonication and boiling protocol. Following the initial pelleting of the bacterial culture, the bacteria cell pellet was first resuspended in 10 mL of Dulbecco's Phosphate Buffered Saline (ThermoFisher) with 50 μ L of 200 mM PMSE. The cell suspension was lysed using a tip sonicator (18% amplitude, 6 pulses of 25 s each with 2 min rest on ice in between pulses) and subsequently immersed in boiling water for 15 min. The bacterial lysate was centrifuged at 10,000 $\times g$ for 10 min at 4 °C and the supernatant was carefully collected. The supernatant was filtered through a 0.22 μ m PES filter (FroggaBio) and purified with the same two-step anion exchange procedure used in the osmotic shock protocol.

To generate nucleic acid-free preparations, following the centrifugation step, 10% streptomycin sulfate dissolved in dH₂O (136 μ L/mL of supernatant) and glacial acetic acid (228 μ L/mL of supernatant) were added to the supernatant and incubated on ice for 5 min [67]. The solution was then centrifuged at 10,000 $\times g$ for 10 min at 4 °C and the supernatant was carefully collected. The collected supernatant was then filtered and purified as described above. Successful removal of nucleic acids was assessed by measuring the ratio of absorbance at 260:280 nm using a NanoDrop spectrophotometer and by performing agarose gel electrophoresis. For this purpose, 18 μ L of 1 mg/mL α Syn was mixed with 6 \times DNA Gel Loading Dye (ThermoFisher Scientific) and run on a 1.5% agarose gel containing ethidium bromide for 30 min at 100 V in 0.5% TAE buffer. The gel was visualized under UV light.

Commercial His-tagged α Syn monomer

Recombinant full-length human α Syn monomers containing an N-terminal poly-histidine tag were purchased from Impact Biologicals (catalog #301-01).

Pre-SAA processing of α Syn substrates

For dialysis experiments, substrates were loaded into a 10 kDa MWCO Slide-A-Lyzer™ MINI Dialysis device (ThermoFisher Scientific #69574) and placed into a beaker containing 1 L of dH₂O with stirring. The dH₂O was replaced every 30 min for a total of 3 changes. Following dialysis, the substrate concentrations were verified by NanoDrop before use in SAA. For centrifugation experiments, substrates were loaded into a 1.5 mL tube and centrifuged at 12,000 $\times g$ for 30 min at 4 °C. For endotoxin removal, 0.5 mL of 1 mg/mL substrate was loaded into Pierce High Capacity Endotoxin Removal Spin Columns (ThermoFisher Scientific #88276) and processed according to the manufacturer's instructions. Following

all processing steps, α Syn substrate concentrations were verified using a NanoDrop spectrophotometer before use in SAA.

Analysis of α Syn substrates by SDS-PAGE and Native PAGE electrophoresis

The relative purity of the different α Syn substrates was assessed by performing standard SDS-PAGE using 10% Bolt Bis–Tris Plus gels. To assess the assembly state of the recombinant α Syn substrates 18 μ L of 1 mg/mL α Syn was mixed with 4X Native Sample Buffer and run on a 4–16% NativePAGE Bis–Glycine Mini Protein Gel for 1.5 h at 4 °C with a running buffer containing Bis-Tricine at pH 6.4. In both cases, gels were visualized using a Pierce Silver Stain Kit (Thermo Scientific #24612).

Circular dichroism spectroscopy

The four different preparations of recombinant α Syn were normalized to 0.1 mg/mL and dialyzed into 10 mM phosphate buffer pH 7.4 containing 100 mM (NH₄)₂SO₄. Following dialysis, samples were filtered through a 0.22 μ m PES filter (FroggaBio). Circular dichroism measurements were conducted at 22 °C using a JASCO J-715 spectropolarimeter. Spectra were normalized to a blank and smoothed when visualized.

Generation of α Syn preformed fibrils

Preformed fibrils (PFFs) of α Syn were generated as previously described [23, 27, 45]. Two separate batches of PFFs were generated by incubating 500 μ L of 5 mg/mL purified α Syn monomer (obtained using the GST-tagged approach) at 37 °C in a digital heated shaking dry bath or a thermomixer set at 1000 rpm for 5 d. At the end of the 5 days, PFFs were sonicated using the Bioruptor Pico sonicator (Diagenode) for at least 40 cycles of 30 s ON/30 s OFF program to achieve \leq 100 nm sizes. The preparations were then aliquoted to the required volumes (5–100 μ L) and stored at –80 °C. PFFs were further characterized for quality control using transmission electron microscopy (EM) and dynamic light scattering (DLS).

For EM analysis, PFFs were diluted in dH₂O to a final concentration of 20 μ M, with 5 μ L of the PFF mixture loaded onto a carbon-coated copper grid and left to sit for 2 min. Next, samples were fixed with 5 μ L of 4% paraformaldehyde for 1 min, and then the grids were washed with dH₂O for 1 min. Three additional washes with dH₂O were performed. Finally, the PFFs on the grid were stained with 2% uranyl acetate for 1 min. The uranyl acetate was removed and then the grids were air dried for 30 min. Images were acquired using a Tecnai Spirit transmission electron microscope as described previously [6]. For DLS analysis, 0.5–1 mg/mL α -syn PFFs solution was prepared by dilution in 0.1 μ m-filtered PBS and centrifugation at 13,000 rpm for 5 min. The supernatant

was transferred to a DLS cuvette and analyzed using the Zetasizer Nano S system (Malvern Panalytical).

α Syn seed amplification assays: unseeded and PFF-seeded
Recombinant α Syn (0.1 mg/mL) was incubated at 37 °C in 100 μ L of reaction buffer (250 mM sodium citrate tribasic dihydrate pH 8.5, 80 μ M SDS, 10 μ M ThT in ddH₂O). All components in the reaction mix including the recombinant α Syn were filtered using 0.2 μ m syringe filters (Basix). Reactions were performed in quadruplicates in black/clear bottom 96-well plates (Corning), and underwent cycles of 29 min rest, 1 min of double orbital shaking at 400 rpm for a total of 100 h. Fluorescence readings were performed every 30 min using an excitation of 440 \pm 10 nm and an emission of 480 \pm 10 nm in a Fluostar Omega or a CLARIOstar microplate reader (BMG Labtech). Gain was manually set at 1,500 and orbital scanning mode was used at 3 mm. In the seeded reactions, 2.22 μ L of 0.05 mg/mL PFFs were added to each 100 μ L of overall reaction mixture. Sodium citrate buffer was compared to multiple other buffers that are commonly used and tested in unseeded vs seeded conditions including: citrate buffer at higher and lower concentrations (500 mM, 250 mM, and 125 mM), PIPES buffer (100 mM PIPES pH 6.5, 300 mM sodium chloride, 80 μ M SDS, 10 μ M ThT in dH₂O), PBS buffer (80 μ M SDS, 10 μ M ThT in PBS pH 7.4), and NaCl at different concentrations (300/150/75 mM NaCl, 80 μ M SDS, and 10 μ M ThT in dH₂O). A minimum of four technical replicates were analyzed per sample.

Preparation and analysis of brain homogenates

Brain homogenates (BHs) from non-transgenic C57BL/6 mice or frozen samples from neuropathologically-confirmed human MSA, DLB, or control cases [10% (w/v) prepared in calcium- and magnesium-free PBS] were generated using a Minilys homogenizer and CK14 soft tissue homogenizing tubes (Bertin Corp.). The MSA samples were obtained from the temporal cortex of a 66-year-old female and a 60-year-old female. The DLB samples were from the temporal cortex of a 79-year-old female and a 62-year-old male with Braak Lewy Body Stage 6 and 5 pathology, respectively. The control sample was from the temporal cortex of a 63-year-old male. Homogenates were aliquoted and stored at -80 °C.

For detergent insolubility assays, 10% BH was added to 10X detergent buffer [5% (v/v) Nonidet P-40, 5% (w/v) sodium deoxycholate in DPBS] containing Halt Phosphatase Inhibitor (ThermoFisher Scientific #78420) and Pierce Universal Nuclease (ThermoFisher Scientific #88701), and chilled on ice for 20 min with vortexing every 5 min. The mixture was centrifuged at 5000 \times g for 5 min at 4 °C to remove debris, and the protein concentration in the supernatant was determined by the

bicinchoninic acid (BCA) assay (ThermoFisher Scientific #23227). Samples were diluted to 1 mg/mL total protein concentration with 1X detergent buffer and ultracentrifuged in a TLA-55 rotor at 100,000 \times g for 1 h at 4 °C. Pellets were resuspended in loading buffer and heated to 95 °C for 10 min.

For thermolysin digestions, detergent-extracted brain homogenates were generated as described above. Samples were digested with 50 μ g/mL thermolysin (MilliporeSigma #T7902) for a protease/protein (w/w) ratio of 1:100. After shaking at 600 rpm. at 37 °C for 1 h, digestions were stopped by adding EDTA to a final concentration of 5 mM. The insoluble fraction was collected by ultracentrifugation and resuspended as described above.

Immunoblotting

Samples were run on 10% Bolt Bis-Tris Plus gels (Thermo Scientific) at 165 V for 42 min. Proteins were transferred onto a 0.45 μ m-pore polyvinylidene fluoride membrane in transfer buffer [25 mM Tris-HCl pH 8.3, 0.192 M glycine, 20% (v/v) methanol] at 35 V for 1 h. Proteins were crosslinked to the membrane in 0.4% (v/v) paraformaldehyde (Electron Microscopy Services #15711) in PBS by gentle rocking at 22 °C for 30 min, then rinsed twice with TBST [1X TBS containing 0.05% (v/v) Tween-20]. Membranes were then incubated in blocking buffer [5% (w/v) skim milk in TBST] at 22 °C for 1.5 h, then incubated with anti-total α Syn mouse monoclonal Syn-1 antibody (1:10,000 dilution; BD Biosciences, #610786) or an anti-Serine129-phosphorylated α Syn rabbit monoclonal EP1536Y (1:10,000 dilution in blocking buffer; Abcam #ab51253) at 4 °C overnight. Membranes were washed three times with TBST at 22 °C for 10 min each, then incubated at 22 °C for 1 h with horseradish peroxidase-conjugated secondary antibodies (1:10,000 dilution in blocking buffer; Bio-Rad, #172-1011 or #172-1019). After another three TBST washes, membranes were developed using Western Lightning enhanced chemiluminescence Pro (Revvity #NEL122001EA) then exposed to HyBlot CL X-ray film (Thomas Scientific #1141J52).

α Syn seed amplification assays: brain homogenate-seeded

To generate brain-derived seeds, 10% (w/v) BH (in PBS) was centrifuged at 10,000 \times g for 10 min at 4 °C. The supernatant was collected, and the protein concentration in the PBS-soluble fraction was determined using the BCA assay. Reactions were performed in black 96-well plates with a clear bottom (Corning). For the reaction mixture, each well contained 10 μ L of the seed (5 μ g of total protein from the PBS-soluble fraction, diluted in PBS), 20 μ L of 50 μ M ThT (final concentration of 10 μ M), 20 μ L of 0.5 mg/mL monomeric recombinant α Syn (final concentration of 0.1 mg/mL), and 50 μ L of the reaction buffer consisting of 80 mM phosphate buffer pH 8,

350 mM sodium citrate tribasic dihydrate (final concentration of 40 mM phosphate buffer pH 8, 175 mM sodium citrate tribasic dihydrate), and three 0.5 mm silica beads. Plates were sealed and incubated at 42 °C in a CLARI-Ostar microplate reader (BMG Labtech) with cycles of 1 min shaking (400 rpm double orbital) and 1 min rest for a period of 48 h. ThT fluorescence measurements (450 ± 10 nm excitation and 480 ± 10 nm emission, bottom read) were taken every 2 min. Four technical replicates were analyzed per sample.

Intact protein mass spectrometry (LC–MS)

As previously described [61], protein samples were diluted to 0.1 mg/mL in 0.1% (v/v) formic acid before 1 µg of each was injected onto a Dionex Ultimate 3000 UHPLC system at 200 µL/min using a Waters Bio-Resolve RP mAb Polyphenyl column (450 Å, 2.7 µM, 2.1 × 100 mm). The resulting eluate (5 min wash with 4% (v/v) acetonitrile in 0.1% (v/v) formic acid, followed by 20 min gradient to 90% (v/v) acetonitrile in 0.1% (v/v) formic acid) was analyzed on an Impact II QTOF mass spectrometer (Bruker Daltonics) equipped with an Apollo II ion funnel electrospray ionization source and Bruker OtofControl v4.0 / DataAnalysis v4.3 software. Following calibration (ESI-L Low Concentration Tuning Mix; Agilent Technologies #G1969-85000), data were acquired in positive-ion profile mode using a capillary voltage of 4,500 V and dry nitrogen heated at 200 °C. Total ion chromatograms were used to determine where the protein eluted, and spectra were summed over the entire elution peak. Multiply charged ion species were deconvoluted at 10,000 resolution using the maximum entropy method.

Analytical ultracentrifugation

The polymeric state of αSyn generated by multiple preparation protocols was analyzed by sedimentation velocity analysis. Samples were diluted to a concentration of 1 mg/mL in water (PBS for GST-tagged αSyn monomer) and then loaded into standard 12 mm 2-sector Epon-charcoal centrifuge cells. Analysis was performed at 10 °C in a Beckman Optima AUC analytical ultracentrifuge. Sedimentation behavior resulting from a rotor speed of 50,000 rpm (An-60 Ti rotor) was observed using the optical absorbance of each sample ($A_{280\text{nm}}$). For each sample, two hundred radial scans were obtained at 3-min intervals. Following calculation of temperature-corrected sample and fluid parameters using the SEDNTERP software package [55], datasets were fitted according to the continuous c(S) Lamm equation model in the SEDFIT software package (version 9.4) [62] to obtain the concentration distribution by sedimentation rate.

Analysis of seed amplification assay data

The unseeded and seeded kinetic curves were fit to a sigmoidal dose–response (variable slope) model in GraphPad Prism to obtain values for the Hill slope (k) and the time at which fluorescence is halfway between the baseline and plateau values (T_{50}). Lag phases were then calculated using the equation $T_{50} - [1/(2*k)]$ [2]. For samples that did not aggregate within the 100 h time-frame, they were assigned a lag time of 100 h. For samples that aggregated immediately, they were given a lag phase of 0 h. The ThT_{Max} values are the highest single value reported for each individual well. Coefficient of variation (CV) was calculated by the formula $CV = \frac{\sigma}{\mu}$, where σ is the standard deviation of the lag time for independent quadruplicate replicates and μ is the mean of the lag time for the same replicates.

Statistical analysis

All statistical analyses were performed using GraphPad Prism (v.9.3) with a significance threshold of $P=0.05$. Data comparisons were made using either one-way ANOVA with Tukey's multiple comparisons test, Welch's ANOVA with Dunnett T3 multiple comparisons test, two-way ANOVA test with Šidák multiple comparisons test, a Kruskal–Wallis test followed by Dunn's multiple comparisons test, or two-tailed unpaired t-tests. In experiments where the values were restricted to an upper limit (lag time), non-parametric tests were used. A semilog non-linear regression was used to analyze the relationship between lag time and PFF seeding amount. Values are reported as mean ± SEM.

Results

We compared four different preparations of recombinant full-length human αSyn for their viability as SAA substrates. Three of the αSyn preparations were produced “in house”, which permits greater flexibility and scalability. Recombinant αSyn monomers were purified either by fusion to a GST tag followed by purification using glutathione beads and removal of the GST tag (“GST-tagged αSyn monomer”: GTM); by bacterial lysis via sonication and boiling followed by anion exchange chromatography (“sonication and boiling αSyn monomer”: SBM); or by bacterial lysis via osmotic shock followed by anion exchange chromatography (“osmotic shock αSyn monomer”: OSM). A schematic of the three recombinant αSyn preparation methods is shown in Additional File 1: Fig. S1. The fourth preparation was obtained from a commercial source and contained an N-terminal poly-histidine tag (“commercial His-tagged αSyn monomer”: CHM).

Osmotic shock-purified α Syn monomer exhibits limited *de novo* aggregation

The spontaneous aggregation propensity of the four different preparations of α Syn was tested via unseeded SAA reactions. Separate batches of the four substrates were tested at two different laboratories to ensure inter-laboratory reliability of the findings and assess the variability of the substrates (Fig. 1a, b). The GTM substrate showed the fastest *de novo* aggregation rate, as determined by having the shortest lag time (Fig. 1c). Notably, the lag time for OSM substrate was longer than for the other three substrates, indicating that it exhibits the lowest propensity for spontaneous aggregation. ThT_{Max} values may correlate with either the structure of the aggregates formed at the end of the reaction or the extent of aggregation. The ThT_{Max} values for OSM were significantly lower than for the other three substrates, congruent with the lack of *de novo* aggregation seen with this substrate (Fig. 1d). Only two of the 16 OSM replicates showed any aggregation, whereas 11/16 SBM, 12/16 CHM and all 16 GTM wells showed aggregation (defined as a lag time of less than 100 h). All five of the SBM wells which did not aggregate were reported at a single lab, suggesting interlab

variability. For the two OSM wells in which α Syn aggregation was apparent, the aggregation occurred near the end of the 100 h incubation period (83.8 h and 95.0 h). To further probe the utility of the OSM substrate, we tested multiple additional batches purified at different times in unseeded reactions and saw similar resistance to *de novo* aggregation across all batches (Fig. 1e). This indicates that low *de novo* aggregation potential is a robust, consistent property of OSM.

One potential explanation for the differences in *de novo* aggregation potential displayed by the four substrates is that the buffer the substrates are stored in is not the same. To address this possibility, all substrates were dialyzed into dH_2O prior to SAA. In unseeded SAA reactions, OSM still performed the best, and the dialysis step did not improve the performance of the other three substrates (Additional File 1: Fig. S2a–d). Similarly, the presence of trace levels of pre-existing α Syn oligomers/aggregates in the substrate could potentially act as a seed in the unseeded SAA reactions. To investigate this potential explanation, the four substrates were centrifuged prior to use in unseeded SAA reactions. Following this centrifugation step, OSM once again exhibited the lowest

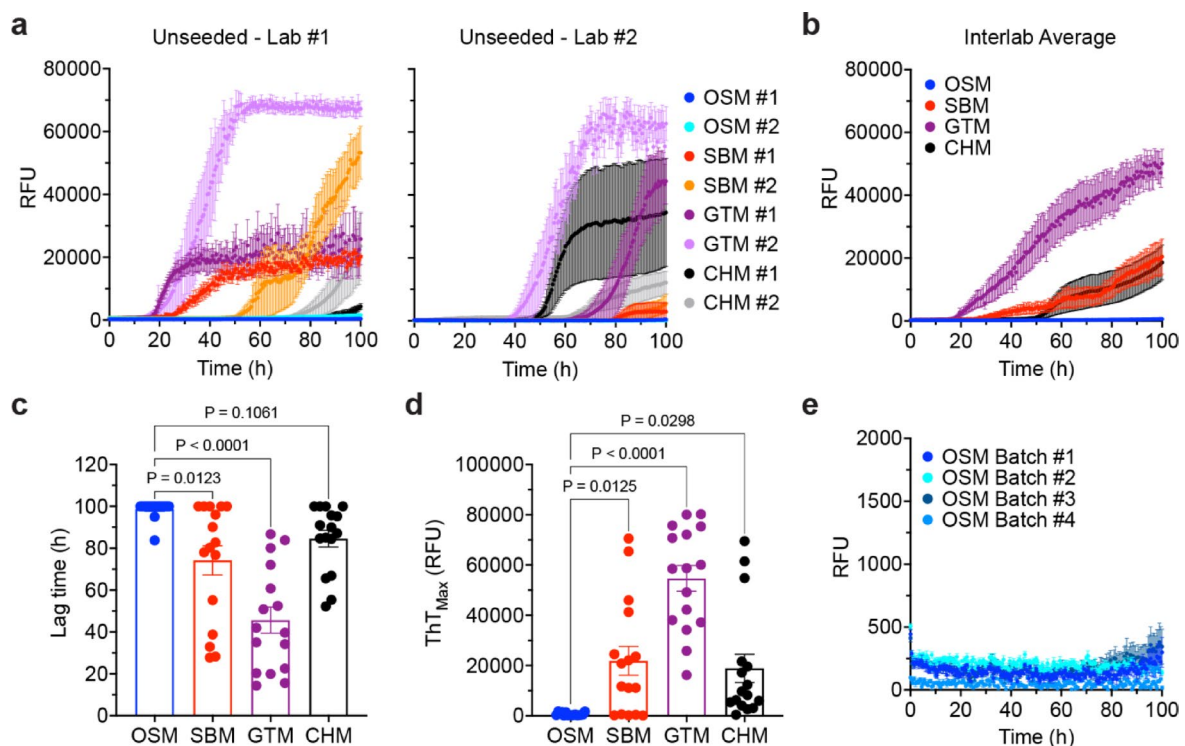


Fig. 1 Spontaneous aggregation kinetics of different monomeric α Syn SAA substrates. **a** ThT aggregation curves for unseeded SAA reactions using either Osmotic Shock Monomer (OSM), Sonicated and Boiled Monomer (SBM), GST-Tagged Monomer (GTM), or Commercially available His-tagged Monomer (CHM). Samples were run in quadruplicates twice in two different labs to ensure inter-laboratory replicability of the results (n=8 replicates per lab). **b** ThT aggregation curves for unseeded SAA reactions using the four α Syn substrates, averaged to generate inter-laboratory results (n=16 total replicates). **c, d** Comparison of the lag times (**c**) and ThT_{Max} values (**d**) for all unseeded reactions (n=16). Lag times were compared using a Kruskal–Wallis test followed by Dunn's multiple comparisons test whereas ThT_{Max} values were compared using Welch's ANOVA test with Dunnett's T3 multiple comparisons test. **e** ThT aggregation curves for unseeded SAA reactions utilizing four independent preparations of OSM (n=4 replicates per batch). All data are mean \pm SEM

spontaneous aggregation potential, and the spontaneous aggregation propensity of the other three substrates was not significantly improved (Additional File 1: Fig. S2e–h). As an additional quality control step, the in-house produced substrates were tested for endotoxin. The SBM substrate tested positive for endotoxins, whereas the other substrates did not. To eliminate this potential confound, we subjected the substrates to an endotoxin removal protocol before using them in unseeded SAA reactions. Following endotoxin removal, OSM was still the best substrate, and none of the other three substrates exhibited a reduced propensity for spontaneous aggregation (Additional File 1: Fig. S2i–l). Thus, the OSM substrate is intrinsically less prone to spontaneous aggregation than the SBM, GTM, and CHM substrates.

Seeding of α Syn monomer preparations with α Syn preformed fibrils

Following analysis of the *de novo* aggregation potential of the four preparations, we examined whether they could be used for the sensitive and specific detection of α Syn preformed fibril (PFF) seeds in SAA. The PFFs were generated using GTM α Syn monomer and the successful formation of fibrils was verified using transmission electron microscopy and dynamic light scattering (Additional File 1: Fig. S3). To compare the performance for each of the

four recombinant α Syn substrates in PFF-seeded SAA reactions, 10^{-3} dilutions of PFFs (from the same batch) were chosen to seed the reactions and tested at both laboratories. As with the unseeded reactions, the same kinetic parameters were assessed. Seeding was apparent with all four α Syn substrates when tested at both laboratories (Fig. 2a, b). In PFF-seeded SAA reactions, the OSM substrate yielded significantly longer lag times than the SBM and GTM substrates (Fig. 2c). ThT_{Max} values were not significantly different between any of the four substrates (Fig. 2d).

When comparing the lag times for the unseeded reactions to the PFF-seeded reactions, the GTM substrate had the smallest difference between unseeded and seeded reactions of 29.8 h, while the OSM (57.5 h), SBM (50.8 h) and CHM (55.6 h) all had larger differences between unseeded and seeded reactions (Fig. 3a, b). These differences were all significant (Fig. 3b). Therefore, while all four types of recombinant α Syn preparations are potentially viable substrates for PFF-seeded SAA reactions, OSM and CHM may be better suited for discriminating between spontaneous aggregation and PFF-induced seeding. We note that PFF-seeded SAA reactions using OSM substrate produced a biphasic aggregation curve (Fig. 3a). This may potentially indicate the occurrence of

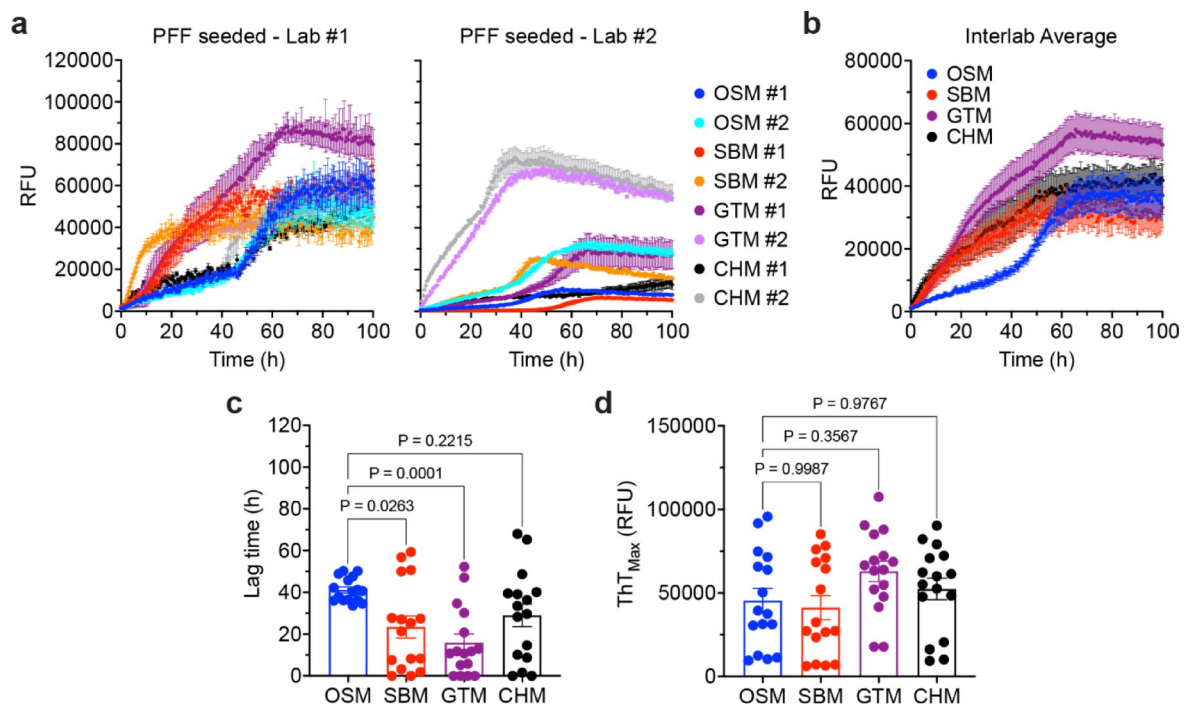


Fig. 2 α Syn substrate performance in PFF-seeded SAA reactions. **a** ThT aggregation curves for SAA reactions seeded with a 10^{-3} dilution of α Syn PFFs using either Osmotic Shock Monomer (OSM), Sonicated and Boiled Monomer (SBM), GST-Tagged Monomer (GTM), or Commercially available His-tagged Monomer (CHM). Samples were run in quadruplicates twice in two different labs to ensure inter-laboratory replicability of the results ($n=8$ replicates per lab). **b** ThT aggregation curves for PFF-seeded SAA reactions using the four α Syn substrates, averaged to generate inter-laboratory results ($n=16$ total replicates). **c, d** Comparison of the lag times (**c**) and ThT_{Max} values (**d**) for all PFF-seeded reactions ($n=16$). Lag times and ThT_{Max} values were compared using Welch's ANOVA test with Dunnett's T3 multiple comparisons test. All data are mean \pm SEM

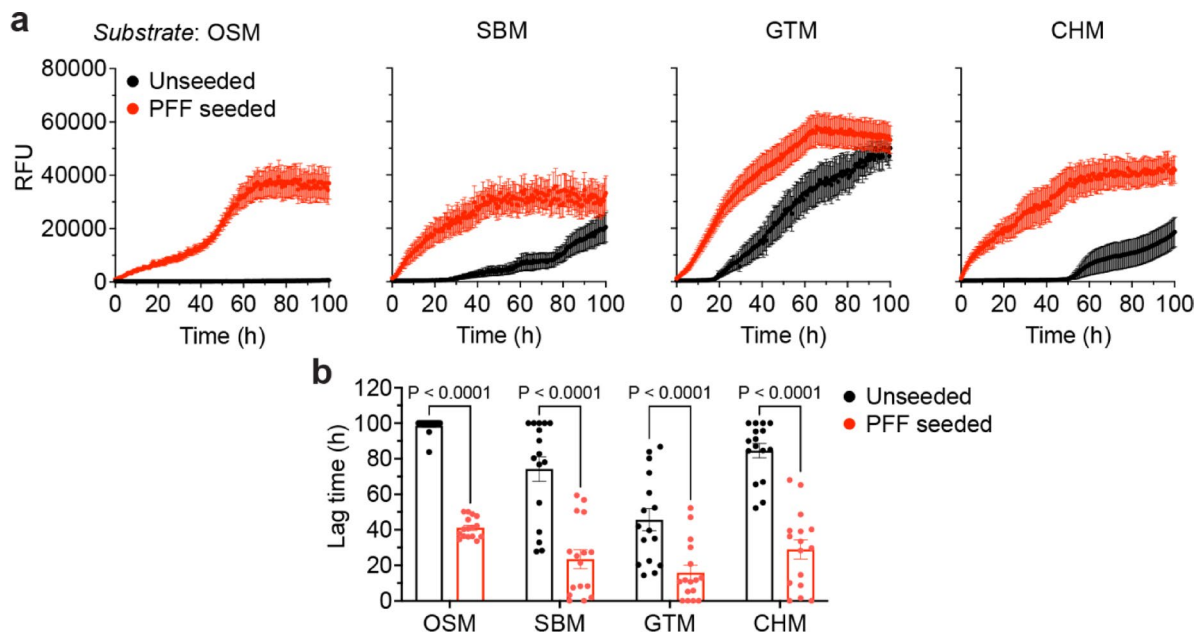


Fig. 3 Comparison of unseeded and PFF-seeded SAA reactions. **a** Overlay of the ThT aggregation curves for the unseeded and PFF-seeded experiments ($n = 16$ per condition). **b** Comparison of the lag times for unseeded and PFF-seeded assays using each of the four recombinant α Syn substrates. To assess statistical significance, samples were compared using two-way ANOVA followed by a Šidák multiple comparisons test. All data are mean \pm SEM

both fibril elongation and surface-mediated (secondary) nucleation [28].

To determine the recombinant α Syn substrate that would be the best for SAA, we examined the inter-experiment variability for both unseeded and PFF-seeded reactions. For the SBM and GTM substrates, both the unseeded and PFF-seeded reactions showed substantial differences in the mean lag times indicating inter-plate variability (Fig. 4a). In comparison, the OSM substrate showed only minor differences between the average lag times of the unseeded reactions, and no substantial differences between individual plates in the PFF-seeded reactions. In both PFF-seeded and unseeded reactions, the CHM substrate exhibited less plate-to-plate variability than the SBM and GTM substrates but greater variability than the OSM substrate. To provide a more quantitative comparison of intra-plate variability between the four substrates, the coefficient of variation (CV) was compared between the unseeded and PFF-seeded reactions. The CV measures the amount of variation in the lag times for each of the independent experiments. The greater the CV the greater the variation within an individual experiment (i.e., greater intra-plate variability in lag time). In both unseeded and PFF-seeded SAA reactions, the OSM substrate had the lowest average CV across experimental replicates (Fig. 4b). In summary, limited inter- and intra-plate variability was observed with the OSM substrate while maintaining a significant difference between the lag times for PFF-seeded and unseeded

reactions, a combination of properties not observed for the other substrates.

Next, we examined the relative sensitivities of the various α Syn substrates in SAA by seeding with a tenfold dilution series of α Syn PFFs. For OSM and CHM, there was a strong direct correlation between the dose of PFFs added and the resultant lag time, with higher PFF dilutions resulting in significantly longer lag times in SAA (Fig. 5a, b, Additional File 1: Fig. S4). In contrast, only a moderate relationship was observed for the SBM and GTM substrates. It should be noted that for lower amounts of PFF seed (10^{-5} and 10^{-6} dilutions), only OSM enabled unambiguous differentiation between seeded aggregation in PFF-seeded reactions and spontaneous aggregation in unseeded reactions (Fig. 5a). Thus, OSM is the most sensitive and specific recombinant α Syn substrate for SAAs.

It has been widely reported that buffer conditions can affect the seeding response in α Syn SAAs [48]. Therefore, we sought to investigate whether OSM's low *de novo* aggregation potential was a consistent property of the purified protein or due to the buffer conditions and experimental setup. If OSM is inherently resistant to *de novo* seeding, then unseeded reactions should follow similar trends regardless of buffer choice. To investigate this issue, we performed unseeded and PFF-seeded SAA reactions with a variety of different buffer conditions using OSM as the substrate. OSM exhibited limited changes in unseeded reactions across the eight buffer conditions tested, suggesting low *de novo* aggregation

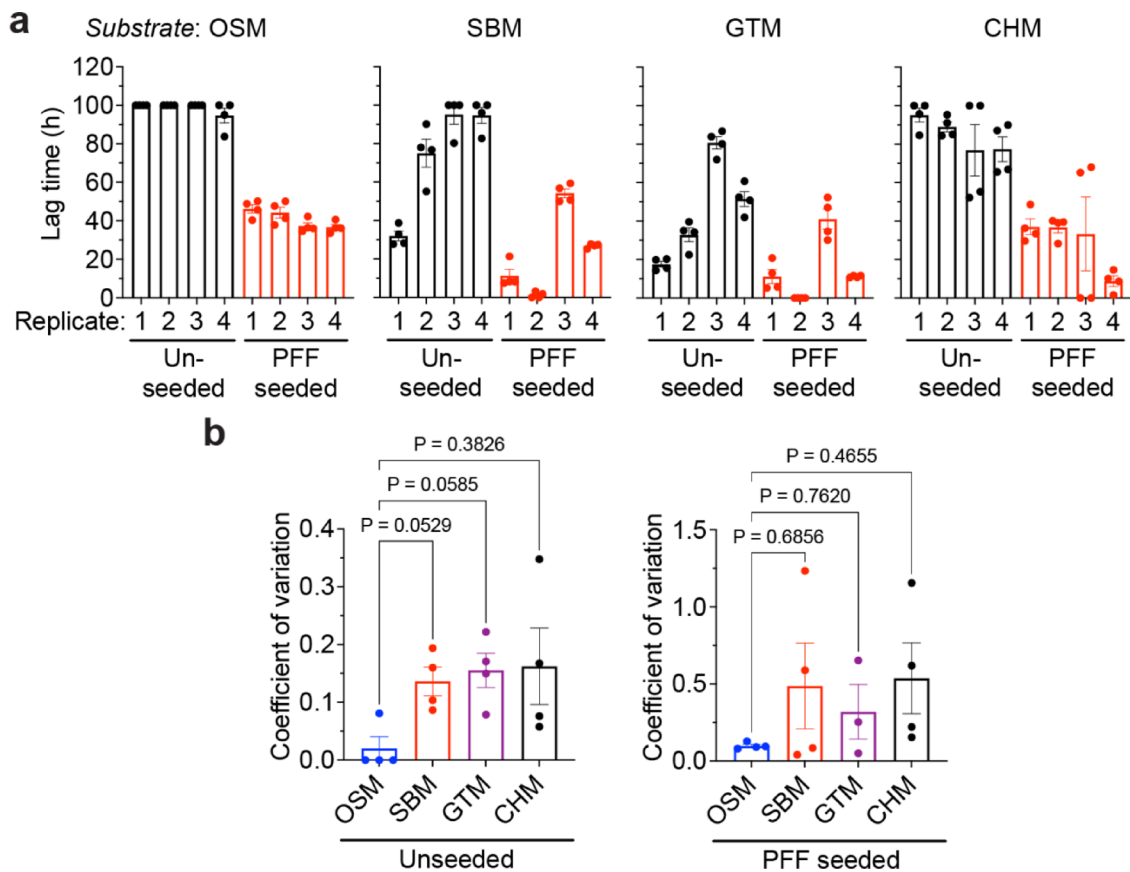


Fig. 4 Substrate variability for unseeded and PFF-seeded SAA reactions. **a** Comparison of the lag times for the four independent replicate unseeded and PFF-seeded SAA experiments, each consisting of quadruplicate reactions, using the four different α Syn substrates to determine the extent of inter-plate variability. **b, c** The coefficient of variation was calculated for each of the independent experiments for both unseeded and seeded reactions for each substrate to determine the amount of intra-plate variability. Statistical significance was assessed using Welch's ANOVA test with Dunnett's T3 multiple comparisons test. All data are mean \pm SEM

propensity is a consistent property of the OSM substrate (Additional File 1: Fig. S5). However, PFF-seeded reactions showed significant variation between buffers, suggesting seeded reactions are highly susceptible to changes in buffer conditions. Nonetheless, several buffers permitted PFF-seeded SAA reactions to be distinguished from unseeded reactions when using OSM substrate.

Specificity of seeding in brain homogenate SAA is dependent on α Syn substrate

As SAAs have been increasingly used for diagnosing synucleinopathies, we next tested the four recombinant α Syn substrates in reactions seeded with brain homogenate (BH), a biologically relevant seed source. BH from the temporal cortex of two MSA cases and two DLB cases were assessed, with BH from a control case without neuropathological changes serving as a negative control. As expected, detergent-insoluble and thermolysin-resistant α Syn species that are phosphorylated at Serine-129 (PSyn), which are indicators of α -syn aggregates [38], were only present in MSA and DLB BH (Fig. 6a).

PBS-soluble fractions were generated for each BH and then tested by SAA using each of the four α Syn substrates. For SAA reactions seeded with MSA or DLB BH, only OSM substrate yielded lag times that were significantly shortened compared to those for reactions seeded with control BH (Fig. 6b–f). For reactions utilizing SBM, GTM, and CHM substrates, the lag times for MSA and DLB BH overlapped substantially with those for reactions seeded with control BH, possibly suggesting that something in human BH non-specifically stimulates the aggregation of these α Syn substrates. Differences in the ThT_{Max} value in SAAs seeded with biospecimens from different human synucleinopathies have been inferred to indicate the presence of structurally distinct α Syn aggregates in the original samples [64]. Therefore, we compared the ThT_{Max} values attained for SAA reactions seeded with MSA or DLB BH for each of the four α Syn substrates. For OSM, GTM, and CHM substrates, SAA reactions seeded with MSA BH produced significantly higher ThT fluorescence than reactions seeded with DLB BH (Fig. 6b, d, e, g). These results are consistent with other studies that

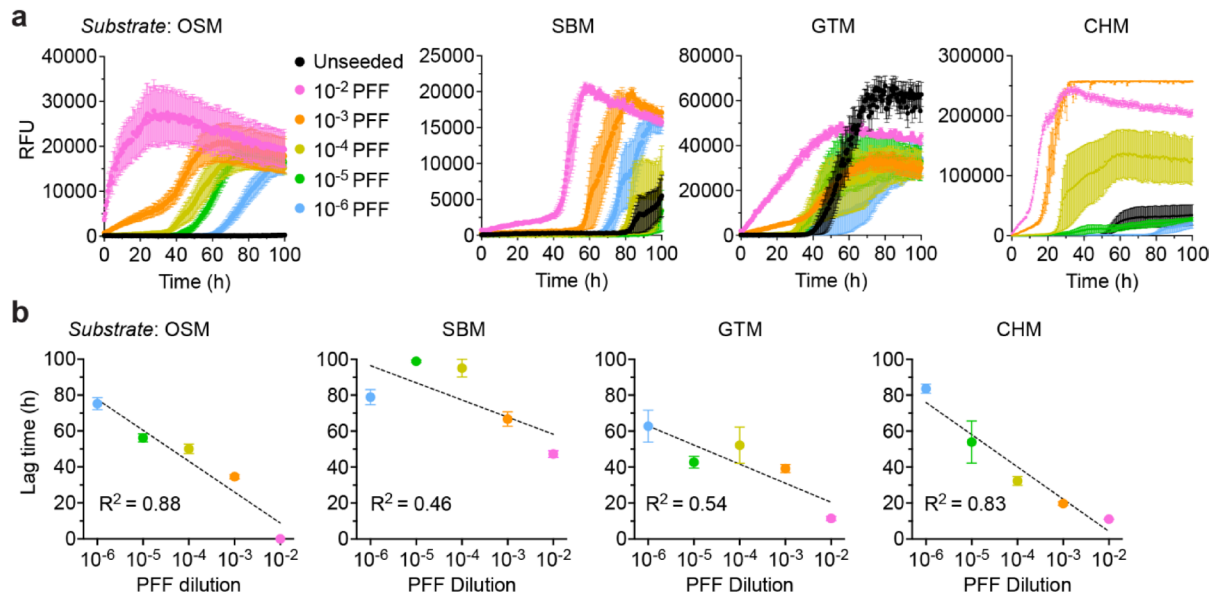


Fig. 5 Dose-dependent detection of α Syn PFF seeds using SAA with OSM substrate. **a** ThT aggregation curves for SAA reactions utilizing each of the four recombinant α Syn substrates seeded with α Syn PFF doses ranging from 10^{-2} to 10^{-6} . The experiment was performed twice with four replicates per experiment for OSM and once with four replicates for the other three substrates. **b** Graphs depicting semilog linear regression analysis for the relationship between PFF dose and lag time for each of the four substrates. Correlation was assessed quantitatively by calculating the R^2 value for each substrate. All data are mean \pm SEM

also utilized a sodium citrate-based buffer that enhances amplification of MSA biospecimens by SAA [39, 48]. Thus, OSM provides the most suitable substrate for synucleinopathy BH SAA as it both distinguishes MSA and DLB cases from a control as well as MSA from DLB.

Characterization of α Syn substrate preparations

To explore potential explanations for their variable performance in the SAA experiments, the recombinant α Syn substrates were analyzed by SDS-PAGE followed by silver staining. The OSM, GTM and SBM substrates all showed a single band at ~ 16 kDa corresponding to full-length α Syn (Fig. 7a). The GTM substrate showed a single band at ~ 17 kDa, with the additional molecular weight likely corresponding to the remnants of the N-terminal linker residues to the GST-tag. A Native PAGE gel was also run to assess the assembly state of each substrate. Like the SDS-PAGE gel, the substrates each showed a single band upon silver staining, with the SBM and OSM migrating at an apparent molecular weight of ~ 21 kDa (Fig. 7b). The higher apparent weight of the CHM substrate is likely due to the N-terminal His-tag which increases both the molecular weight and charge of the protein in Native PAGE. To attempt to assess if different native structures of the substrates could be impacting performance in SAA, we next measured the circular dichroism (CD) spectra of the proteins to look for differences in secondary structure. The CD spectra of the GTM, SBM, and CHM substrates were consistent with random coil structure, with local minima around 200 nm (Fig. 7c).

However, the OSM substrate showed a distinct right shift and broadening of the peak which may suggest some level of α -helical structure. OSM substrate had a significantly higher wavelength of the minima compared to all other substrates (CHM: 196.4; GTM: 199.5; SBM: 200.0; OSM: 204.9) (Fig. 7d).

We also analyzed OSM, SBM, GTM and CHM substrates using intact protein mass spectrometry and analytical ultracentrifugation to further understand potential differences that may explain differences in SAA performance. Mass spectrometry analysis showed high consistency in expected mass values for different batches across the different purification methods (Fig. 8a). For each sample set, purity was consistent across both batches and the deconvoluted masses correlated well the expected amino acid sequences (<1 Dalton tolerance): OSM (theoretical: 14,460.2; observed: 14,459.4); SBM (theoretical: 14,460.2; observed: 14,459.4); CHM, (theoretical: 15,584.4 – Met1 = 15,453.2; observed: 15,452.4); GTM, (theoretical: 14,871.6; observed: 14,870.9). Notably, the sonicated ‘SBM’ batches contained an extra peak at 14,704.7 (+245.3 mass shift) which was not present in the OSM batches. Common to bacterial expression, loss of the initiator methionine (-131.2 mass shift) and a minor secondary peak at 15,630.6 (expected +178.2 gluconoylation of His-tag) were detected for the CHM batches.

In analytical ultracentrifugation experiments, all monomers showed a main sedimentation peak at the approximate molecular weight expected for each

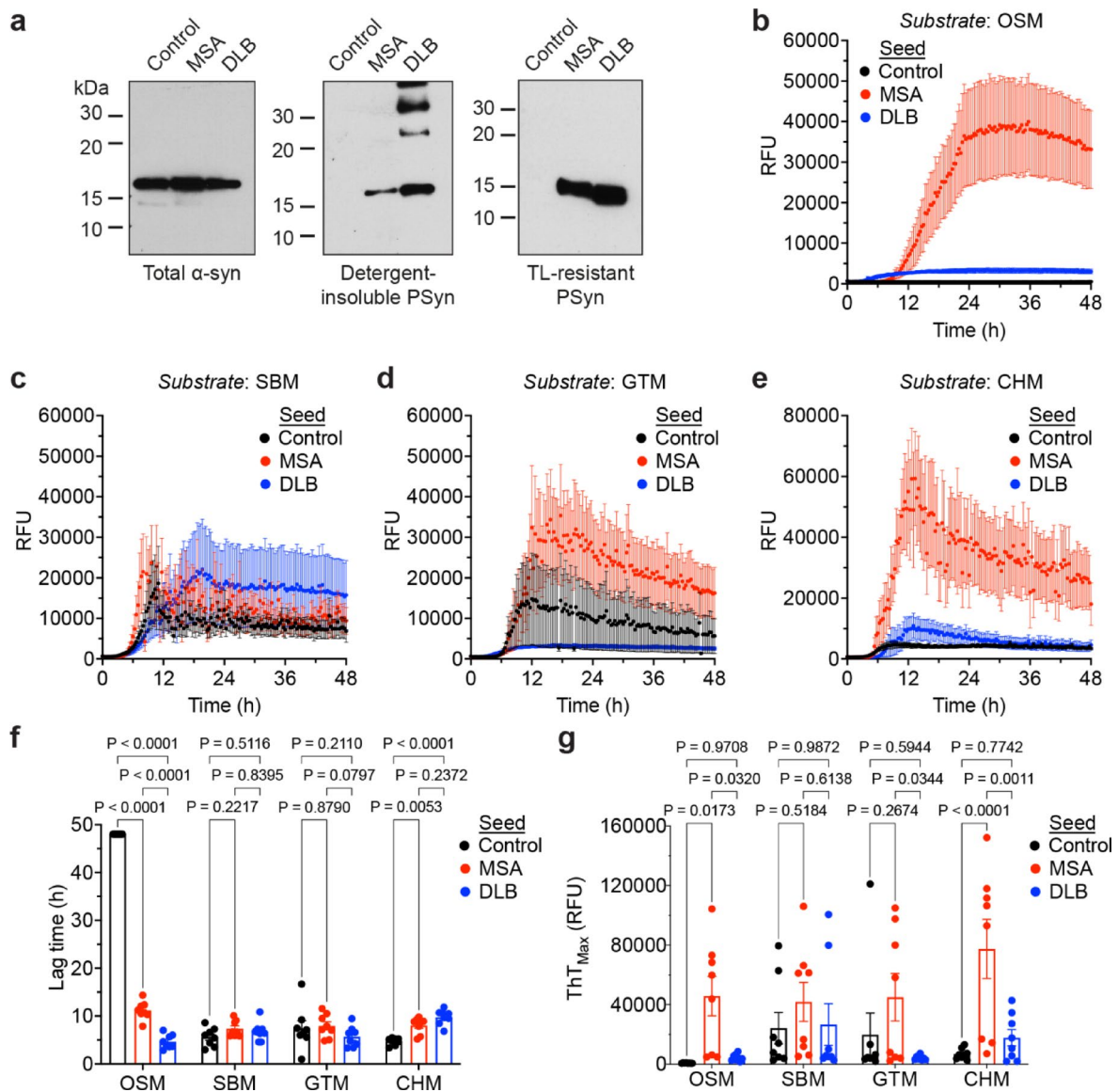


Fig. 6 α Syn substrate performance in SAA reactions seeded with synucleinopathy brain homogenate. **a** Immunoblots of total α Syn, detergent-insoluble Serine-129 phosphorylated α Syn (PSyn) species, and detergent-insoluble thermolysin (TL)-resistant PSyn species in brain homogenates from MSA, DLB, and control human cases. Total α -syn was detected with the antibody Syn-1 and PSyn was detected using the antibody EP1536Y. **b–e** ThT aggregation curves for SAA reactions utilizing each of the four α Syn substrates seeded with the PBS-soluble fraction from MSA ($n = 2$), DLB ($n = 2$), or control ($n = 1$) BH. Each MSA and DLB sample was analyzed in quadruplicate whereas 8 replicates were performed for the control sample. Data for the 2 MSA cases and the 2 DLB were pooled to generate a single curve for each disease. **f, g** Comparison of the lag times (**f**) and ThT_{Max} values (**g**) for the BH-seeded reactions ($n = 8$). Statistical significance was assessed using two-way ANOVA followed by a Šidák multiple comparisons test. All data are mean \pm SEM

protein sequence (OSM: 14.4 kDa; GTM: 14.7 kDa; SBM: 14.6 kDa; CHM: 16.4 kDa) (Fig. 8b). However, on three separate runs using two separate batches of OSM, a minor peak ($\sim 15\%$ of sample) corresponding to a higher molecular weight (~ 45 kDa) species was noted. This species was not observed in any of the other monomer preparations. This may reflect a tendency for OSM to form multimeric structures that are more resistant to aggregation in SAA leading to a lower *de novo* seeding propensity. However, deeper and more systemic analyses

are required to understand the relevance and structural composition of these conformations.

It was noted based on 260:280 nm absorbance ratios and verified by agarose gel electrophoresis that SBM substrate contains nucleic acid contamination that is absent in the OSM substrate (Additional File 1: Fig. S6a, b). Modification of the SBM purification protocol to remove nucleic acid (SBM-NA) reduced the propensity for *de novo* aggregation in unseeded reactions (Additional File 1: Fig. S6c). However, in BH-seeded SAA reactions,

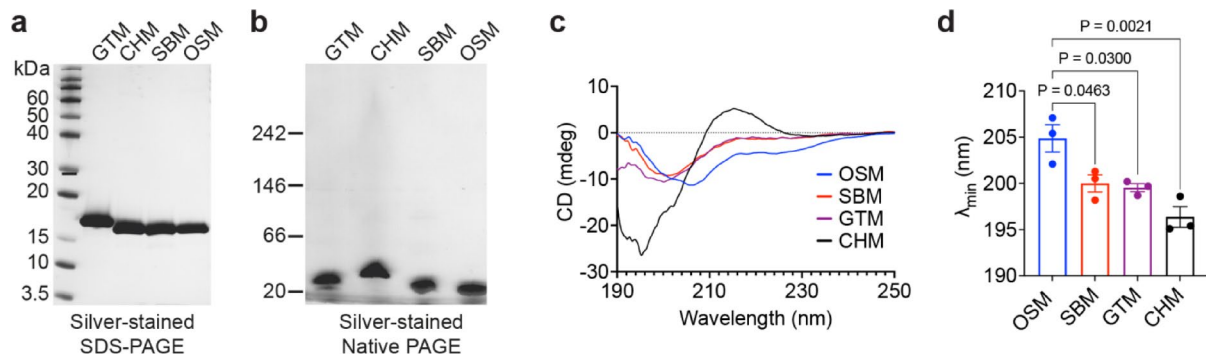


Fig. 7 Comparison of α Syn substrate properties. **a** All four substrates (15 μ g protein loaded per lane) were analyzed by SDS-PAGE followed by silver staining to assess potential protein contamination. **b** All four substrates (15 μ g protein loaded per lane) were analyzed by Native PAGE followed by silver staining to assess the assembly state of the substrates. **c** CD spectra for each of the four α Syn substrates ($n=3$ batches per substrate). **d** Comparison of the wavelength minima in the CD spectra for OSM, SBM, GTM, and CHM substrates. Data are mean \pm SEM. Statistical significance was assessed using one-way ANOVA with Tukey's multiple comparisons test

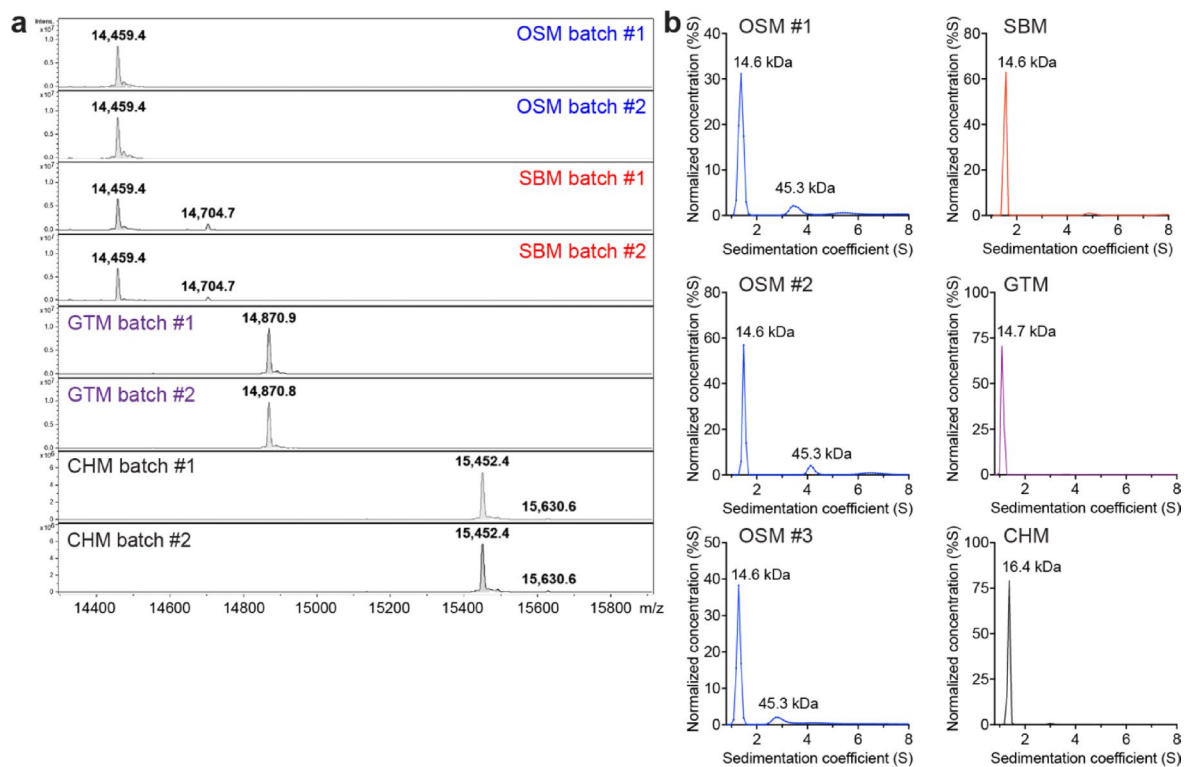


Fig. 8 Mass spectrometry and analytical ultracentrifugation analysis of α Syn substrates. **a** Two batches each of OSM, SBM, GTM and CHM were analyzed using LC-MS to look for the presence of post-translational modifications. **b** Sedimentation velocity analysis of two batches of OSM (over 3 runs) and one run each of SBM, GTM and CHM substrates were analyzed using absorbance optics. Concentration values were normalized using the sum of all values to enable comparisons of samples across different runs. Sedimentation coefficient values were plotted from 0.5 to 8.0 S and calculated molecular weights are shown

SBM-NA did not show the same level of discrimination as OSM (Additional File 1: Fig. S6d, e). This suggests that some, but not all, of the higher *de novo* aggregation propensity of SBM can be attributed to nucleic acid contamination and that other factors must also contribute to the superior performance of OSM substrate in SAA.

Discussion

As the use of α Syn SAAs continues to increase, so too does the need to standardize conditions between labs and to understand the potential impact different protocols can have on the results. In fact, researchers have recently been emphasizing the need for standardization of protocols since SAAs notoriously suffer from high variability [1, 8, 10, 37, 44]. This variability can

have significant implications on the validity of the assay results for different biospecimens, especially as SAAs begin to move towards adoption in the clinical realm. To this end, we tested four recombinant α Syn substrate preparation methods for their viability to be used in SAA and compared the results obtained across two laboratories. The OSM substrate always displayed the most consistent results across all ThT kinetic parameters tested in unseeded and seeded reactions. Interestingly, limited batch-to-batch variability in OSM substrate has been reported by other groups when using cerebrospinal fluid as the seed for SAA [44]. These properties make OSM the ideal substrate for SAA as it reduces the rates of false positive reactions, while still allowing high sensitivity in seeded reactions and a high degree of intra- and inter-laboratory reliability.

As a substrate, GTM was not suited for SAA as it had the fastest *de novo* aggregation rate of all substrates tested, leading to false positive reactions that would make seeded reactions difficult to interpret. Moreover, GTM was found to be the fastest aggregating substrate in both laboratories, showing a high degree of intra- and inter-laboratory replicability. Interestingly, the CHM and SBM substrates both showed significant inter-laboratory variability. In one laboratory, the CHM substrate aggregated extremely quickly making it unsuitable for SAA, whereas the SBM substrate showed a low aggregation propensity comparable to OSM. However, the other laboratory found the exact opposite, with the SBM being a fast-aggregating substrate compared to the slow-aggregating CHM. It has been noted in the literature that some preparations of His-tagged α Syn monomer can produce “slow” or “fast” kinetic batches of substrate [12]. This further supports the idea that batch-to-batch variability in certain preparations of substrate can be a significant concern in SAA [37, 44]. Variability is particularly important to consider when testing biological samples, as this may increase the rates of false positives or negatives if an assay was optimized using a “fast” kinetic batch but later run with a “slow” kinetic batch, or vice versa. Similarly, the choice of buffer conditions and cycle settings are pivotal in the final seeding kinetics achieved. Changing the buffer while using OSM had a significant impact on lag time and well-to-well variability in PFF-seeded reactions. Therefore, it may be prudent to characterize the kinetics of each batch of substrate prior to further use.

Our in-house prepared OSM substrate was able to reveal differences in ThT kinetics between BH from MSA and DLB cases. This suggests that OSM as a substrate can be used in biologically relevant applications and replicate results that were generated with other preparations of substrate (typically CHM). While the differences in ThT_{Max} support the hypothesis that MSA and DLB are caused by distinct α Syn strains, it is important

to note that the structures of α -syn aggregates generated *in vitro* by seeded reactions using MSA and PD/DLB biospecimens as a template are distinct from those obtained directly from synucleinopathy patient brains [24, 40, 63, 81]. Whether OSM substrate may permit better conformational fidelity when amplifying patient-derived α Syn aggregates remains to be determined.

In an attempt to understand why the various recombinant α Syn substrates behaved differently in the SAA, we explored multiple possibilities. As the behavior of SBM and OSM substrates, which both consist of full-length untagged wild-type human α Syn, were different, we think it is unlikely that simple sequence difference could explain seeding differences observed. Furthermore, as the four substrates each displayed a single band following SDS-PAGE and single peaks following LC-MS, we do not believe that protein contamination is a likely explanation. Therefore, it is likely that there are other contributing factors. Dialysis and centrifugation of substrates prior to SAA did not appreciably modify SAA performance, nor did removal of endotoxin. Thus, pre-existing trace amounts of α Syn aggregates are unlikely to explain the divergent performance of the substrates in SAA, although we cannot rule out the existence of low amounts of soluble oligomeric α Syn species in the SBM, CHM, and GTM (but not OSM) preparations that could act as seeds. Potential nucleic acid contamination was noted in the SBM preparations and given that it has been reported that DNA can enhance fibrillization of α Syn via direct interactions [19, 32], this provided a plausible explanation for the *de novo* aggregation propensity of SBM. However, nucleic acid contamination was only noted in SBM and would not explain the spontaneous aggregation propensities of CHM and GTM. Moreover, while nucleic acid-free SBM substrate did exhibit a reduced propensity for spontaneous aggregation, it still did not perform as well in BH-seeded SAA reactions as OSM. Given the variability between SBM batches, it is possible that the nucleic acid-free SBM simply represents one extreme of this batch-to-batch variability, and that the nucleic acid removal was inconsequential. Nonetheless, it is conceivable that an as-yet-undetected minor contaminant, such as a lipid species, in one or more of the α Syn substrates could provide an explanation for variable performance in SAA.

A unique biophysical property of the OSM substrate was that the peak of the CD spectra was right shifted compared to the other substrates. We speculate that this could indicate some proportion of α -helical content in the OSM not present in the other substrates. This shift in the CD spectra of OSM compared to the other substrates mirrors the CD spectra changes noted in tetrameric compared to monomeric α Syn by other groups [5, 77]. Additionally, using analytical ultracentrifugation,

we noted that OSM preparations contain a minor species with a higher molecular weight, raising the possibility that OSM α Syn monomers may exist in equilibrium with higher-order structures. Most groups have found that α Syn exists as an unstructured monomer when not bound to membranes [26]. However, others have documented the existence of tetrameric α -helical α Syn species that, unlike monomeric unstructured α Syn, are aggregation-resistant [5, 77]. However, this resistance to aggregation only applied to *de novo* aggregation, as tetrameric α Syn could still be seeded as effectively as monomeric α Syn. Tetrameric α Syn can undergo a temperature-dependent irreversible-dissociation, which may explain why SBM is a poor substrate for SAA, as the boiling step in the purification would likely destroy tetrameric α Syn species [5, 77]. The presence of either an N-terminal poly-histidine tag or the residual N-terminal sequence 'GPLGS' following cleavage of the GST-tag in CHM and GTM, respectively, could alter either the ability of α Syn to form aggregation-resistant tetramers or their equilibrium with monomeric α Syn, which could hinder their use in SAA. Finally, previous work involving purification of tetrameric α Syn used non-denaturing conditions, similar to the OSM protocol, which could imply that tetrameric α Syn species are preserved in OSM. While this is an attractive theory, the Native PAGE gel does not support it, as the apparent molecular weight of the OSM, which we speculate could contain tetramers, and the SBM, which we speculate does not contain tetramers, was the same. However, given the fragile nature of tetramers, it is possible that the tetramers dissociate during the sample preparation for Native PAGE.

Another potential explanation for the differential substrate behaviors may be the oxidation state of α Syn. It has previously been reported that α Syn can become oxidized on its four methionine residues, resulting in the formation of methionine sulfoxides [30, 76]. Oxidized α Syn has a lower *de novo* aggregation propensity compared to unoxidized α Syn [76]. Osmotic shock is often called periplasmic lysis, as it selectively harvests proteins from the periplasmic space as opposed to the cytosol [29, 75]. However, the reported changes in CD spectra of oxidized α Syn are not identical to what we found for the OSM substrate [76]. In addition, mass spectrometry analysis did not indicate the presence of oxidation in two separate purifications of OSM. A further challenge to this hypothesis is that previous papers reporting "fast" and "slow" kinetic recombinant α Syn batches use a modified osmotic shock procedure. However, that study used His-tagged α Syn, which may be a confounding factor given that we observed variable results with our CHM substrate [12]. This is further supported as the CHM used in this study was also produced via a modified osmotic shock procedure and similarly showed two very different

kinetic profiles between the batches tested in each lab. It is also possible the explanation for why each different substrate did not perform as well may not be a common factor and instead could be due to unique factors specific to each purification method.

Conclusion

As the field continues towards the use of α Syn SAA for the diagnosis and prognosis of synucleinopathies, care must be taken in the optimization and design of these assays to ensure intra- and inter-laboratory reproducibility. This is especially important as these technologies begin their transition into the commercial and clinical realms. In this work, we demonstrate that the method used to purify the α Syn substrate can dramatically impact its SAA performance. We therefore strongly encourage the use of OSM as the universal substrate for α Syn SAA.

Abbreviations

α Syn	α -Synuclein
PD	Parkinson's disease
MSA	Multiple system atrophy
DLB	Dementia with Lewy bodies
SAA	Seed amplification assays
ThT	Thioflavin T
AD	Alzheimer's disease
GTM	GST-tagged α Syn monomer
SBM	Sonication and boiling α Syn monomer
OSM	Osmotic shock α Syn monomer
CHM	Commercial His-tagged α Syn monomer
BH	Brain homogenate
CV	Coefficient of variation
CD	Circular dichroism

Supplementary Information

The online version contains supplementary material available at <https://doi.org/10.1186/s40478-025-02151-4>.

Supplementary Material 1

Acknowledgements

The authors thank Mark A. Hancock (McGill SPR-MS Facility) for assistance with the intact protein LC-MS analyses, for which infrastructure was gratefully provided by the Canada Foundation for Innovation (CFI). The authors thank Kim Munro, staff scientist at the centre de recherche en biologie structurale, for conducting the analytical ultracentrifugation analysis, which was funded by Fonds de Recherche du Québec (Health Sector) Research Centres Grant #288558.

Author contributions

ZAMA and NRGs contributed equally to the collection, analysis, and interpretation of all results included within the manuscript. SM conducted the biochemical analysis on patient brain extracts. SN aided in the performance and optimization of OSM purification methodology. CS assisted with the nucleic acid-free SBM purification. GTM purification and PFF generation were performed by WL. Electron microscopy characterization and dynamic light scattering analyses were performed by WL and IS, respectively. MI and BTH generously provided the brain homogenate samples used in this study. JFT led the mass-spectrometry and ultracentrifugation result analyses and interpretation for all α Syn substrates. GTM and PFF batches were kindly provided by TMD. ZAMA, NRGs, JCW and EAF were responsible for the study conception and design. First draft was written by ZAMA and NRGs. All authors read and approved the final manuscript.

Funding

This work was funded by grants to EAF from Parkinson Canada and the Canadian Institutes of Health Research (PJT-195804) and to JCW from the Canadian Institutes of Health Research (PJT-169042). EAF, JCW, and TMD acknowledge the support of the Government of Canada's New Frontiers in Research Fund (NFRF), NFRFT-2022-00051. EAF is supported by a Canada Research Chair (Tier 1) in Parkinson's disease and JCW is supported by a Canada Research Chair (Tier 2) in protein misfolding disorders. NRGs was supported by doctoral fellowships funded in partnership between Parkinson Canada and the Parkinson Society of British Columbia (GSA-2022-000000100), a CIHR Canadian Graduate Scholarship Doctoral Research Award (514557) as well as an Ontario Graduate Scholarship. ZAMA was supported by the Judi Richardson Parkinson Canada Pilot Grant (ID: PPG-2023-000000139) and the Canadian Institutes of Health Research doctoral Vanier Canada Graduate Scholarship (CGS-D) (FRN: CGV-186893).

Data availability

All data generated or analysed during this study are included in this published article and its supplementary information files. Raw SAA kinetic curves can be made available upon reasonable request from the corresponding authors.

Declarations

Ethics approval and consent to participate

Human α -synucleinopathy samples were provided by the Massachusetts Alzheimer's Disease Research Center. Informed consent was obtained either by the patient prior to death or by family member prior to or at the time of death. The use of human tissue was in accordance with guidelines provided by the University of Toronto under an approved human participant ethics protocol (#38879; "Use of human tissue for research on neurodegenerative diseases"), and all relevant ethical regulations were followed.

Consent for publication

Not applicable.

Competing interests

The authors declare no competing interests.

Author details

¹Department of Neurology and Neurosurgery, Montreal Neurological Institute-Hospital (The Neuro), McGill University, 3801 University Street, Montreal, QC H3A 2B4, Canada

²Tanz Centre for Research in Neurodegenerative Diseases, University of Toronto, 60 Leonard Ave, Toronto, ON M5T 0S8, Canada

³Department of Biochemistry, University of Toronto, Toronto, ON, Canada

⁴The Neuro's Early Drug Discovery Unit (EDDU), Montreal Neurological Institute, McGill University, Montreal, QC, Canada

⁵Krembil Brain Institute, University Health Network, Toronto, ON, Canada

⁶Department of Laboratory Medicine and Pathobiology, University of Toronto, Toronto, ON, Canada

⁷Department of Medicine, University of Toronto, Toronto, ON, Canada

⁸Rudbeck Laboratory, Department of Public Health/Geriatrics, Uppsala University, Uppsala, Sweden

⁹Department of Neurology, Massachusetts General Hospital, Charlestown, MA, USA

¹⁰Department of Radiology, Massachusetts General Hospital, Charlestown, MA, USA

¹¹Neuroscience Program, Harvard Medical School, Boston, MA, USA

¹²Department of Pharmacology and Therapeutics and Centre de Recherche en Biologie Structurale, McGill University, Montreal, QC, Canada

Received: 7 May 2025 / Accepted: 8 October 2025

Published online: 05 November 2025

References

1. Al-Azzawi M, Konig A, Outeiro TF (2022) Production of recombinant Alpha-synuclein: still no standardized protocol in sight. *Biomolecules*. <https://doi.org/10.3390/biom12020324>

- Arosio P, Knowles TP, Linse S (2015) On the lag phase in amyloid fibril formation. *Phys Chem Chem Phys* 17:7606–7618. <https://doi.org/10.1039/c4cp05563b>
- Bargar C, De Luca CMG, Devigili G, Elia AE, Cilia R, Portaleone SM et al (2021) Discrimination of MSA-P and MSA-C by RT-QuIC analysis of olfactory mucosa: the first assessment of assay reproducibility between two specialized laboratories. *Mol Neurodegener* 16:82. <https://doi.org/10.1186/s13024-021-00491-y>
- Bargar C, Wang W, Gunzler SA, LeFevre A, Wang Z, Lerner AJ et al (2021) Streamlined alpha-synuclein RT-QuIC assay for various biospecimens in Parkinson's disease and dementia with Lewy bodies. *Acta Neuropathol Commun* 9:62. <https://doi.org/10.1186/s40478-021-01175-w>
- Bartels T, Choi JG, Selkoe DJ (2011) Alpha-synuclein occurs physiologically as a helically folded tetramer that resists aggregation. *Nature* 477:107–110. <http://doi.org/10.1038/nature10324>
- Bayati A, Ayoubi R, Aguila A, Zorca CE, Deyag G, Han C et al (2024) Modeling Parkinson's disease pathology in human dopaminergic neurons by sequential exposure to α -synuclein fibrils and proinflammatory cytokines. *Nat Neurosci* 27:2401–2416. <https://doi.org/10.1038/s41593-024-01775-4>
- Bellomo G, De Luca CMG, Paoletti FP, Gaetani L, Moda F, Parnetti L (2022) Alpha-synuclein seed amplification assays for diagnosing synucleinopathies: the way forward. *Neurology* 99:195–205. <https://doi.org/10.1212/WNL.000000000000200878>
- Bellomo G, Paciotti S, Gatticchi L, Rizzo D, Paoletti FP, Fragai M et al (2021) Seed amplification assays for diagnosing synucleinopathies: the issue of influencing factors. *Front Biosci (Landmark Ed)* 26:1075–1088. <https://doi.org/10.52586/5010>
- Bentivenga GM, Mammana A, Baiardi S, Rossi M, Ticca A, Magliocchetti F et al (2024) Performance of a seed amplification assay for misfolded alpha-synuclein in cerebrospinal fluid and brain tissue in relation to Lewy body disease stage and pathology burden. *Acta Neuropathol* 147:18. <https://doi.org/10.1007/s00401-023-02663-0>
- Bernhardt AM, Nemati M, Boros FA, Hopfner F, Levin J, Mollenhauer B et al (2024) Alpha-synuclein seed amplification assays from blood-based extracellular vesicles in Parkinson's disease: an evaluation of the evidence. *Mov Disord* 39:1269–1271. <https://doi.org/10.1002/mds.29923>
- Bongianni M, Ladogana A, Capaldi S, Klotz S, Baiardi S, Cagnin A et al (2019) Alpha-synuclein RT-QuIC assay in cerebrospinal fluid of patients with dementia with Lewy bodies. *Ann Clin Transl Neurol* 6:2120–2126. <https://doi.org/10.1002/acn3.50897>
- Brauer S, Rossi M, Sajapin J, Henle T, Gasser T, Parchi P et al (2023) Kinetic parameters of alpha-synuclein seed amplification assay correlate with cognitive impairment in patients with Lewy body disorders. *Acta Neuropathol Commun* 11:162. <https://doi.org/10.1186/s40478-023-01653-3>
- Brauer S, Weber M, Deuschle C, Julia K, Concha-Marambio L, Bernhardt AM et al (2025) High agreement across laboratories between different Alpha-synuclein seed amplification protocols. *Eur J Neurol* 32:e70165. <https://doi.org/10.1111/ene.70165>
- Brockmann K, Lerche S, Baiardi S, Rossi M, Wurster I, Quadalti C et al (2024) CSF alpha-synuclein seed amplification kinetic profiles are associated with cognitive decline in Parkinson's disease. *NPJ Parkinsons Dis* 10:24. <https://doi.org/10.1038/s41531-023-00627-5>
- Brockmann K, Quadalti C, Lerche S, Rossi M, Wurster I, Baiardi S et al (2021) Association between CSF alpha-synuclein seeding activity and genetic status in Parkinson's disease and dementia with Lewy bodies. *Acta Neuropathol Commun* 9:175. <https://doi.org/10.1186/s40478-021-01276-6>
- Bsoul R, McWilliam OH, Waldemar G, Hasselbalch SG, Simonsen AH, von Buchwald C et al (2025) Accurate detection of pathologic alpha-synuclein in CSF, skin, olfactory mucosa, and urine with a uniform seeding amplification assay. *Acta Neuropathol Commun* 13:113. <https://doi.org/10.1186/s40478-025-02034-8>
- Bsoul R, Simonsen AH, Frederiksen KS, Svenstrup K, Bech S, Salvesen L et al (2025) Seeding amplification assay with universal control fluid: standardized detection of alpha-synucleinopathies. *PLoS ONE* 20:e0326568. <https://doi.org/10.1371/journal.pone.0326568>
- Candelise N, Schmitz M, Llorens F, Villar-Pique A, Cramm M, Thom T et al (2019) Seeding variability of different alpha synuclein strains in synucleinopathies. *Ann Neurol* 85:691–703. <https://doi.org/10.1002/ana.25446>
- Cherry D, Hoyer W, Subramaniam V, Jovin TM (2004) Double-stranded DNA stimulates the fibrillation of alpha-synuclein in vitro and is associated with the mature fibrils: an electron microscopy study. *J Mol Biol* 344:929–938. <https://doi.org/10.1016/j.jmb.2004.09.096>

20. Concha-Marambio L, Pritzkow S, Shahnawaz M, Farris CM, Soto C (2023) Seed amplification assay for the detection of pathologic alpha-synuclein aggregates in cerebrospinal fluid. *Nat Protoc* 18:1179–1196. <https://doi.org/10.1038/s41596-022-00787-3>
21. Coughlin DG, Shifflett B, Farris CM, Ma Y, Galasko D, Edland SD et al (2025) Alpha-Synuclein seed amplification assay amplification parameters and the risk of progression in prodromal Parkinson disease. *Neurology* 104:e210279. <https://doi.org/10.1212/WNL.000000000000210279>
22. De Luca CMG, Elia AE, Portaleone SM, Cazzaniga FA, Rossi M, Bistaffa E et al (2019) Efficient RT-QuIC seeding activity for alpha-synuclein in olfactory mucosa samples of patients with Parkinson's disease and multiple system atrophy. *Transl Neurodegener* 8:24. <https://doi.org/10.1186/s40035-019-0164-x>
23. Del Cid Pellitero E, Shlaifer R, Luo W, Krahn A, Nguyen-Renou E, Manecka D-L et al (2019) Quality control characterization of α -synuclein preformed fibrils (PFFs). *City*
24. Dhavale DD, Barclay AM, Borcik CG, Basore K, Berthold DA, Gordon IR et al (2024) Structure of alpha-synuclein fibrils derived from human Lewy body dementia tissue. *Nat Commun* 15:2750. <https://doi.org/10.1038/s41467-024-46832-5>
25. Fairfoul G, McGuire LI, Pal S, Ironside JW, Neumann J, Christie S et al (2016) Alpha-synuclein RT-QuIC in the CSF of patients with alpha-synucleinopathies. *Ann Clin Transl Neurol* 3:812–818. <https://doi.org/10.1002/acn3.338>
26. Fauvet B, Mbefo MK, Fares MB, Desobry C, Michael S, Ardah MT et al (2012) Alpha-Synuclein in central nervous system and from erythrocytes, mammalian cells, and *Escherichia coli* exists predominantly as disordered monomer. *J Biol Chem* 287:15345–15364. <https://doi.org/10.1074/jbc.M111.318949>
27. Feller B, Fallon A, Luo W, Nguyen PT, Shlaifer I, Lee AK et al (2023) α -Synuclein preformed fibrils bind to β -neurexins and impair β -neurexin-mediated presynaptic organization. *Cells* 12:1083
28. Gaspar R, Meisl G, Buell AK, Young L, Kaminski CF, Knowles TPJ et al (2017) Secondary nucleation of monomers on fibril surface dominates alpha-synuclein aggregation and provides autocatalytic amyloid amplification. *Q Rev Biophys* 50:e6. <https://doi.org/10.1017/S0033583516000172>
29. Giehm L, Lorenzen N, Otzen DE (2011) Assays for alpha-synuclein aggregation. *Methods* 53:295–305. <https://doi.org/10.1016/j.jymeth.2010.12.008>
30. Glaser CB, Yamin G, Uversky VN, Fink AL (2005) Methionine oxidation, alpha-synuclein and Parkinson's disease. *Biochim Biophys Acta* 1703:157–169. <https://doi.org/10.1016/j.bbapap.2004.10.008>
31. Groveman BR, Orru CD, Hughson AG, Raymond LD, Zanusso G, Ghetti B et al (2018) Rapid and ultra-sensitive quantitation of disease-associated alpha-synuclein seeds in brain and cerebrospinal fluid by alphaSyn RT-QuIC. *Acta Neuropathol Commun* 6:7. <https://doi.org/10.1186/s40478-018-0508-2>
32. Hegde ML, Vasudevaraju P, Rao KJ (2010) DNA induced folding/fibrillation of alpha-synuclein: new insights in Parkinson's disease. *Front Biosci (Landmark Ed)* 15:418–436. <https://doi.org/10.2741/3628>
33. Hoglinger GU, Adler CH, Berg D, Klein C, Outeiro TF, Poewe W et al (2024) A biological classification of Parkinson's disease: the SynNeurGe research diagnostic criteria. *Lancet Neurol* 23:191–204. [https://doi.org/10.1016/S1474-4422\(23\)00404-0](https://doi.org/10.1016/S1474-4422(23)00404-0)
34. Huang C, Ren G, Zhou H, Wang CC (2005) A new method for purification of recombinant human alpha-synuclein in *Escherichia coli*. *Protein Expr Purif* 42:173–177. <https://doi.org/10.1016/j.pep.2005.02.014>
35. Iranzo A, Fairfoul G, Ayudhaya ACN, Serradell M, Gelpi E, Vilaseca I et al (2021) Detection of alpha-synuclein in CSF by RT-QuIC in patients with isolated rapid-eye-movement sleep behaviour disorder: a longitudinal observational study. *Lancet Neurol* 20:203–212. [https://doi.org/10.1016/S1474-4422\(20\)30449-X](https://doi.org/10.1016/S1474-4422(20)30449-X)
36. Kang UJ, Boehme AK, Fairfoul G, Shahnawaz M, Ma TC, Hutten SJ et al (2019) Comparative study of cerebrospinal fluid alpha-synuclein seeding aggregation assays for diagnosis of Parkinson's disease. *Mov Disord* 34:536–544. <https://doi.org/10.1002/mds.27646>
37. Lashuel HA, Surmeier DJ, Simuni T, Merchant K, Caughey B, Soto C et al (2025) Alpha-synuclein seed amplification assays: data sharing, standardization needed for clinical use. *Sci Adv* 11:eadt7195. <https://doi.org/10.1126/sciadv.aadt7195>
38. Lau A, So RWL, Lau HHC, Sang JC, Ruiz-Riquelme A, Fleck SC et al (2020) Alpha-Synuclein strains target distinct brain regions and cell types. *Nat Neurosci* 23:21–31. <https://doi.org/10.1038/s41593-019-0541-x>
39. Lau HHC, Martinez-Valbuena I, So RWL, Mehra S, Silver NRG, Mao A et al (2023) The G51D SNCA mutation generates a slowly progressive alpha-synuclein strain in early-onset Parkinson's disease. *Acta Neuropathol Commun* 11:72. <https://doi.org/10.1186/s40478-023-01570-5>
40. Lovestam S, Schweighauser M, Matsubara T, Murayama S, Tomita T, Ando T et al (2021) Seeded assembly in vitro does not replicate the structures of alpha-synuclein filaments from multiple system atrophy. *FEBS Open Bio* 11:999–1013. <https://doi.org/10.1002/2211-5463.13110>
41. Ma Y, Farris CM, Weber S, Schade S, Nguyen H, Perez-Soriano A et al (2024) Sensitivity and specificity of a seed amplification assay for diagnosis of multiple system atrophy: a multicentre cohort study. *Lancet Neurol* 23:1225–1237. [https://doi.org/10.1016/S1474-4422\(24\)00395-8](https://doi.org/10.1016/S1474-4422(24)00395-8)
42. Malfertheiner K, Stefanova N, Heras-Garvin A (2021) The concept of alpha-synuclein strains and how different conformations may explain distinct neurodegenerative disorders. *Front Neurol* 12:737195. <https://doi.org/10.3389/fneur.2021.737195>
43. Mammana A, Baiardi S, Quadalti C, Rossi M, Donadio V, Capellari S et al (2021) RT-quick detection of pathological alpha-Synuclein in skin punches of patients with Lewy body disease. *Mov Disord* 36:2173–2177. <https://doi.org/10.1002/mds.28651>
44. Mammana A, Baiardi S, Rossi M, Quadalti C, Ticca A, Magliocchetti F et al (2024) Improving protocols for alpha-synuclein seed amplification assays: analysis of preanalytical and analytical variables and identification of candidate parameters for seed quantification. *Clin Chem Lab Med* 62:2001–2010. <https://doi.org/10.1515/cclm-2023-1472>
45. Maneca D-L, Luo W, Krahn A, Del Cid PE, Shlaifer I, Nicouleanu M et al (2022) Production of recombinant α synuclein monomers and preformed fibrils (PFFs). *Zenodo*. <https://doi.org/10.5281/zenodo.6430401>
46. Manne S, Kondru N, Hepker M, Jin H, Anantharam V, Lewis M et al (2019) Ultrasensitive detection of aggregated alpha-synuclein in glial cells, human cerebrospinal fluid, and brain tissue using the RT-QuIC assay: new high-throughput neuroimmune biomarker assay for parkinsonian disorders. *J Neuroimmune Pharmacol* 14:423–435. <https://doi.org/10.1007/s11481-019-09835-4>
47. Manne S, Kondru N, Jin H, Anantharam V, Huang X, Kanthasamy A et al (2020) Alpha-synuclein real-time quaking-induced conversion in the submandibular glands of Parkinson's disease patients. *Mov Disord* 35:268–278. <https://doi.org/10.1002/mds.27907>
48. Martinez-Valbuena I, Visanji NP, Kim A, Lau HHC, So RWL, Alshimeri S et al (2022) Alpha-synuclein seeding shows a wide heterogeneity in multiple system atrophy. *Transl Neurodegener* 11:7. <https://doi.org/10.1186/s40035-022-00283-4>
49. Mastrangelo A, Caldera S, Mastenbroek SE, Vittoriosi E, Janelidze S, Serrano GE et al (2025) Quantification of Lewy body pathology by cerebrospinal fluid endpoint dilution RT-QuIC in a neuropathological autopsy cohort of clinically heterogeneous participants. *Acta Neuropathol* 149:67. <https://doi.org/10.1007/s00401-025-02904-4>
50. Okuzumi A, Hatano T, Matsumoto G, Nojiri S, Ueno SI, Imamichi-Tatano Y et al (2023) Propagative alpha-synuclein seeds as serum biomarkers for synucleinopathies. *Nat Med* 29:1448–1455. <https://doi.org/10.1038/s41591-023-02358-9>
51. Orru CD, Vaughan DP, Vijaratnam N, Real R, Martinez-Carrasco A, Fumi R et al (2025) Diagnostic and prognostic value of alpha-synuclein seed amplification assay kinetic measures in Parkinson's disease: a longitudinal cohort study. *Lancet Neurol* 24:580–590. [https://doi.org/10.1016/S1474-4422\(25\)00157-7](https://doi.org/10.1016/S1474-4422(25)00157-7)
52. Parveen S, Alam P, Orru CD, Vascellari S, Hughson AG, Zou WQ et al (2025) A same day alpha-synuclein RT-QuIC seed amplification assay for synucleinopathy biospecimens. *NPJ Biosens* 2:8. <https://doi.org/10.1038/s44328-024-00023-w>
53. Paslawski W, Lorenzen N, Otzen DE (2016) Formation and characterization of alpha-synuclein oligomers. *Methods Mol Biol* 1345:133–150. https://doi.org/10.1007/978-1-4939-2978-8_9
54. Perra D, Bongianini M, Novi G, Janes F, Bessi V, Capaldi S et al (2021) Alpha-synuclein seeds in olfactory mucosa and cerebrospinal fluid of patients with dementia with Lewy bodies. *Brain Commun* 3:fcab045. <https://doi.org/10.1093/braincomms/fcab045>
55. Philo JS (2023) SEDNTERP: a calculation and database utility to aid interpretation of analytical ultracentrifugation and light scattering data. *Eur Biophys J* 52:233–266. <https://doi.org/10.1007/s00249-023-01629-0>
56. Poggolini I, Erskine D, Vaikath NN, Ponraj J, Mansour S, Morris CM et al (2021) RT-QuIC using C-terminally truncated α -synuclein forms detects differences in seeding propensity of different brain regions from synucleinopathies. *Biomolecules*. <https://doi.org/10.3390/biom11060820>

57. Poggiolini I, Gupta V, Lawton M, Lee S, El-Turabi A, Querejeta-Coma A et al (2022) Diagnostic value of cerebrospinal fluid alpha-synuclein seed quantification in synucleinopathies. *Brain* 145:584–595. <https://doi.org/10.1093/brain/awab431>
58. Rossi M, Baiardi S, Teunissen CE, Quadalti C, van de Beek M, Mammana A et al (2021) Diagnostic value of the CSF α -synuclein real-time quaking-induced conversion assay at the prodromal MCI stage of dementia with Lewy bodies. *Neurology* 97:e930–e940. <https://doi.org/10.1212/WNL.00000000000012438>
59. Rossi M, Candelise N, Baiardi S, Capellari S, Giannini G, Orru CD et al (2020) Ultrasensitive RT-QulC assay with high sensitivity and specificity for Lewy body-associated synucleinopathies. *Acta Neuropathol* 140:49–62. <https://doi.org/10.1007/s00401-020-02160-8>
60. Russo MJ, Orru CD, Concha-Marambio L, Gaiasi S, Groveman BR, Farris CM et al (2021) High diagnostic performance of independent alpha-synuclein seed amplification assays for detection of early Parkinson's disease. *Acta Neuropathol Commun* 9:179. <https://doi.org/10.1186/s40478-021-01282-8>
61. Saran A, Kim H-M, Manning I, Hancock MA, Schmitz C, Madej M et al (2024) Unveiling the molecular mechanisms of the type IX secretion system's response regulator: structural and functional insights. *PNAS Nexus*. <https://doi.org/10.1093/pnasnexus/pgae316>
62. Schuck P, Perugini MA, Gonzales NR, Howlett GJ, Schubert D (2002) Size-distribution analysis of proteins by analytical ultracentrifugation: strategies and application to model systems. *Biophys J* 82:1096–1111. [https://doi.org/10.1016/S0006-3495\(02\)75469-6](https://doi.org/10.1016/S0006-3495(02)75469-6)
63. Schweighauser M, Shi Y, Tarutani A, Kametani F, Murzin AG, Ghetti B et al (2020) Structures of alpha-synuclein filaments from multiple system atrophy. *Nature* 585:464–469. <https://doi.org/10.1038/s41586-020-2317-6>
64. Shah Nawaz M, Mukherjee A, Pritzkow S, Mendez N, Rabadia P, Liu X et al (2020) Discriminating alpha-synuclein strains in Parkinson's disease and multiple system atrophy. *Nature* 578:273–277. <https://doi.org/10.1038/s41586-020-1984-7>
65. Shah Nawaz M, Tokuda T, Waragai M, Mendez N, Ishii R, Trenkwalder C et al (2017) Development of a biochemical diagnosis of Parkinson disease by detection of alpha-synuclein misfolded aggregates in cerebrospinal fluid. *JAMA Neurol* 74:163–172. <https://doi.org/10.1001/jamaneurol.2016.4547>
66. Simuni T, Chahine LM, Poston K, Brumm M, Buracchio T, Campbell M et al (2024) A biological definition of neuronal alpha-synuclein disease: towards an integrated staging system for research. *Lancet Neurol* 23:178–190. [https://doi.org/10.1016/S1474-4422\(23\)00405-2](https://doi.org/10.1016/S1474-4422(23)00405-2)
67. Singh PK, Kotia V, Ghosh D, Mohite GM, Kumar A, Maji SK (2013) Curcumin modulates alpha-synuclein aggregation and toxicity. *ACS Chem Neurosci* 4:393–407. <https://doi.org/10.1021/cn3001203>
68. So RWL, Watts JC (2023) Alpha-synuclein conformational strains as drivers of phenotypic heterogeneity in neurodegenerative diseases. *J Mol Biol* 435:168011. <https://doi.org/10.1016/j.jmb.2023.168011>
69. Sokratian A, Ziaee J, Kelly K, Chang A, Bryant N, Wang S et al (2021) Heterogeneity in alpha-synuclein fibril activity correlates to disease phenotypes in Lewy body dementia. *Acta Neuropathol* 141:547–564. <https://doi.org/10.1007/s00401-021-02288-1>
70. Soto C (2024) Alpha-Synuclein seed amplification technology for Parkinson's disease and related synucleinopathies. *Trends Biotechnol* 42:829–841. <https://doi.org/10.1016/j.tibtech.2024.01.007>
71. Spillantini MG, Goedert M (2000) The alpha-synucleinopathies: Parkinson's disease, dementia with Lewy bodies, and multiple system atrophy. *Ann N Y Acad Sci* 920:16–27. <https://doi.org/10.1111/j.1749-6632.2000.tb06900.x>
72. Srivastava A, Wang Q, Orru CD, Fernandez M, Compta Y, Ghetti B et al (2024) Enhanced quantitation of pathological alpha-synuclein in patient biospecimens by RT-QulC seed amplification assays. *PLoS Pathog* 20:e1012554. <https://doi.org/10.1371/journal.ppat.1012554>
73. Standke HG, Kraus A (2022) Seed amplification and RT-QulC assays to investigate protein seed structures and strains. *Cell Tissue Res*. <https://doi.org/10.1007/s00441-022-03595-z>
74. Steiner JA, Quansah E, Brundin P (2018) The concept of alpha-synuclein as a prion-like protein: ten years after. *Cell Tissue Res* 373:161–173. <https://doi.org/10.1007/s00441-018-2814-1>
75. Stephens AD, Matak-Vinkovic D, Fernandez-Villegas A, Kaminski Schierle GS (2020) Purification of recombinant alpha-synuclein: a comparison of commonly used protocols. *Biochemistry* 59:4563–4572. <https://doi.org/10.1021/aacs.biochem.0c00725>
76. Uversky VN, Yamin G, Souillac PO, Goers J, Glaser CB, Fink AL (2002) Methionine oxidation inhibits fibrillation of human alpha-synuclein in vitro. *FEBS Lett* 517:239–244. [https://doi.org/10.1016/S0014-5793\(02\)02638-8](https://doi.org/10.1016/S0014-5793(02)02638-8)
77. Wang W, Perovic I, Chittuluru J, Kaganovich A, Nguyen LT, Liao J et al (2011) A soluble alpha-synuclein construct forms a dynamic tetramer. *Proc Natl Acad Sci U S A* 108:17797–17802. <https://doi.org/10.1073/pnas.1113260108>
78. Wang Z, Becker K, Donadio V, Siedlak S, Yuan J, Rezaee M et al (2020) Skin alpha-Synuclein aggregation seeding activity as a novel biomarker for Parkinson disease. *JAMA Neurol* 78:1–11. <https://doi.org/10.1001/jamaneurol.2020.3311>
79. Wiseman JA, Turner CP, Faull RLM, Halliday GM, Dieriks BV (2025) Refining alpha-synuclein seed amplification assays to distinguish Parkinson's disease from multiple system atrophy. *Transl Neurodegener* 14:7. <https://doi.org/10.1186/s40035-025-00469-6>
80. Xue C, Lin TY, Chang D, Guo Z (2017) Thioflavin t as an amyloid dye: fibril quantification, optimal concentration and effect on aggregation. *R Soc Open Sci* 4:160696. <https://doi.org/10.1098/rsos.160696>
81. Yang Y, Shi Y, Schweighauser M, Zhang X, Kotecha A, Murzin AG et al (2022) Structures of alpha-synuclein filaments from human brains with Lewy pathology. *Nature* 610:791–795. <https://doi.org/10.1038/s41586-022-05319-3>

Publisher's Note

Springer Nature remains neutral with regard to jurisdictional claims in published maps and institutional affiliations.